An electrochemical investigation of the dissolution of platinum employing $AlCl_3/HNO_3$

E Medupe

16893867

Dissertation submitted in partial fulfilment of the requirements for the degree *Magister Scientiae* in Chemistry at the Potchefstroom Campus of the North-West University

Supervisor: Dr RJ Kriek

September 2014

DECLARATION

I declare that this dissertation entitled “An electrochemical investigation of the dissolution of platinum employing $AlCl_3$/ HNO_3” is my own work and that it has not been submitted for any degree or examination in any other university, and that all sources I have used or quoted have been indicated and acknowledge by complete references.

Signature …….. **Date ……..**

Acknowledgements

I would like to express my sincere gratitude to the following persons and organizations:

- Dr. R.J. Kriek, my supervisor for the supervision.
- Professor S.W. Vorster for his most valuable input, encouragement and support.
- The Department of Chemistry and Chemical Resource Beneficiation for their assistance.
- The PGM Chemistry Group for their support and for giving me confidence.
- HySA, NRF and North-West University for their financial support.
- The late Johannah Mmapula Medupe, my mum, family at large and friends for their support and believing in me, without them this study would not have been possible.
- Last but not least the Almighty God for the strength and protection he gave me throughout this study.

Thank you all!

Abstract

Industrial activities of mankind are feared to damage the environment irretrievably. Especially the release of huge amounts of harmful gases causes concern. In this regard the environmental pollution caused by the one billion motor vehicles on earth is particularly important. The platinum-group metals (PGM) are well known for their catalytic activity. They are used extensively for reducing the amounts of hydrocarbons, carbon monoxide and nitrogen oxides from the exhausts gas emitted by automobiles. In 2012 20% of platinum and 27% of palladium produced were used in the manufacture of catalytic converters. With the increasing use of PGM-containing autocatalysts, the reclaiming of PGMs from spent catalysts has become essential. Particularly attractive hydrometallurgical methods are those based on the use of halide ions e.g. sodium chloride, as complexing agent in conjunction with nitric acid as oxidant. The chemical reactions between mixtures of aluminium chloride and nitric acid have been studied, but the electrochemical reactions have received little attention. The research reported in this dissertation is aimed at providing data relating to the electrochemical behaviour of platinum in mixtures of aluminium chloride and nitric acid.

The construction of Pourbaix diagrams of platinum in chloride environments confirmed that the stable chloro-complexes $[PtCl_4]^{2-}$ and $PtCl_6]^{2-}$, as well as platinum oxides (PtO and PtO_2) could play a role under the experimental conditions employed in this study. From the thermodynamic results it can be concluded that the systems deserving consideration favour high chloride concentrations and high temperatures.

Notable anodic reactions found were the adsorption of chloride on the platinum surface and the gradual formation of $[PtCl_6]^{2-}$, followed by the formation of platinum oxides at 1.00 to 1.01 V. The results show that anodic currents diminished with lower chloride concentrations. A seemingly anomalous anodic behaviour at 35 °C and 45 °C could be explained in terms of a competition between platinum oxide formation and the formation of platinum chloro-complexes. Evidence for the following cathodic reduction reactions was found: hydrogen evolution, reduction of dissolved oxygen to hydrogen dioxide (-1.3 V SHE), nitrate ion reduction to nitrite ions (-0.01 V SHE), nitrite ion reduction to nitric oxide (-0.85 V SHE) and reduction of PtO and PtO_2 to Pt (at -1.00 V and 1.01 V SHE, respectively).

A brief study was undertaken in an attempt to relate the electrochemical results to the leaching of platinum from a virgin automotive exhaust catalyst. The recovery was low for mixtures with low chloride concentrations, which could be expected from the electrochemical polarisation curves obtained in electrolytes with different chloride concentrations. The maximum platinum recovery attained, was 60% at 45 °C in a mixture containing 0.6 M $AlCl_3$ and 0.9 M HNO_3.

Keywords: platinum, electrochemistry, Pourbaix diagrams, aluminum chloride, nitric acid, leaching

Opsomming

Daar word gevrees dat industriële aktiwiteite van die mensdom besig is om die omgewing onherroeplik te beskadig. Veral die vrylating van groot hoeveelhede skadelike gasse veroorsaak kommer. In hierdie verband is die besoedeling van die omgewing wat veroorsaak word deur die een miljard motorvoertuie op aarde veral belangrik. Die platinum-groep metale (PGM) is bekend vir hul katalitiese aktiwiteit. Hulle word algemeen gebruik vir die vermindering van die hoeveelhede koolwaterstowwe, koolstofmonoksied en stikstofoksiedes in die uitlaatgasse van motorvoertuie. In 2012 is 20% van die geproduseerde platinum en 27% van palladium gebruik in die vervaardiging van katalitiese omsetters. Met die toenemende gebruik van PGM-bevattende uitlaat-katalisatore, het die herwinning van PGM'e uit gebruikte katalisatore noodsaaklik geword. Besonder aantreklike hidrometallurgiese herwinningsmetodes word gebaseer op die gebruik van haliedione (vanaf bv natriumchloried) as komplekseermiddels in samewerking met salpetersuur as oksidant. Die chemiese reaksies in mengsels van aluminiumchloried en salpetersuur is reeds bestudeer, maar die elektrochemiese reaksies het tot dusver min aandag ontvang. Die navorsing in hierdie verhandeling gerapporteer, is gemik op die verskaffing van data met betrekking tot die elektrochemiese gedrag van platinum in mengsels van aluminiumchloried en salpetersuur.

Die konstruksie van Pourbaix-diagramme van platinum in chloriedomgewings het bevestig dat die stabiele chloro-komplekse $[PtCl_4]^{2-}$ en $[PtCl_6]^{2-}$, sowel as die platinumoksiedes (PtO en PtO_2) 'n rol kan speel onder die eksperimentele toestande in hierdie studie. Van die termodinamiese resultate kan afgelei word dat in die stelsels wat oorweeg moet word, hoë chloriedkonsentrasies en hoë temperature in ag geneem moet word.

Noemenswaardige anodereaksies wat gevind is, is die adsorpsie van chloried op die platinum-oppervlak en die geleidelike vorming van $[PtCl_6]^{2-}$, gevolg deur die vorming van platinum-oksiedes by 1.00 tot 1.01 V. Die resultate toon dat anodestrome verminder by laer chloriedkonsentrasies. Oënskynlik teenstrydige anode-gedrag by 35 °C en 45 °C kon verduidelik word in terme van 'n kompetisie tussen die platinum-oksiedvorming en die vorming van platinum-chloro-komplekse. Bewyse is vir die volgende katodiese reduksiereaksies gevind: waterstofontwikkeling, die reduksie van suurstof tot waterstofdioksied (-1.3 V SWE), nitraatioon-

reduksie na nitrietione (-0.01 V SWE), nitrietioon-reduksie tot stikstofoksied (-0.85 V SWE) en die reduksie van PtO en PtO_2 tot Pt (by -1.00 V en 1.01 V SWE, onderskeidelik).

'n Kort studie is onderneem in 'n poging om die elektrochemiese resultate in verband te bring met die loging van platinum uit 'n ongebruikte uitlaat-katalisator. Die herwinning was laag in mengsels met lae chloriedkonsentrasies, wat uit die elektrochemiese polarisasiekrommes van elektroliete met verskillende chloriedkonsentrasies verwag kon word. Die maksimum platinumherwinning was 60% by 45 °C in 'n mengsel bestaande uit 0.6 M $AlCl_3$ en 0.9 M HNO_3.

Kernwoorde: platinum, elektrochemie, Pourbaix diagramme, aluminiumchloried, salpetersuur, loging

Table of contents

List of Figures

List of Tables

List of Symbols

E	Potential (V)
E_a	Activation energy (kJ mol^{-1})
E_e	Equilibrium potential (V)
F	Faraday constant (96 480 C mol^{-1})
j	Current density (A cm^{-2})
j_o	Exchange current density (A cm^{-2})
R	Gas constant (8.314 J mol^{-1} K^{-1})
ΔG	Gibbs free energy change (kJ mol^{-1})
ΔH	Enthalpy (kJ mol^{-1})
η	Overpotential (V)

CHAPTER 1: INTRODUCTION AND BACKGROUND

1.1 Introduction

This study was undertaken against the background of increasing concerns about the state of the atmosphere, which is feared to be damaged irretrievably by the industrial activities of mankind. The growing global consumption of fossil fuels leads to energy-related emissions, which may eventually enhance the greenhouse effect, resulting in climate change with impact on all human activities and natural ecosystems (Fenger 1999). In this regard the platinum group metals (PGMs: platinum, palladium, rhodium, ruthenium, iridium and osmium) are finding important uses in a wide range of technologies to enhance the quality of our lives and lessen the negative impact on the environment. PGMs are installed in catalytic converters to trim down the amount of carbon monoxide (CO), various nitric oxides (NO_x), as well as volatile organic hydrocarbons (VOCs) released into the atmosphere by internal combustion engines. These metals are expensive strategic materials that need to be recycled (Kalavrouziotis and Koukoulakis 2009).

Currently, over half of the world's 1 000 million cars have been equipped with catalytic converters. This was done to meet the increasingly stringent legal limits set by governments in order to attain acceptable functionality of emission systems and presently heavy trucks, buses and construction vehicles are also equipped with autocatalysts (Fornalczyk *et al.* 2009; Sousanis 2011)

1.2 PGM recovery and recycling

The platinum group metals are preferred as active catalytic materials for three reasons: (1) these metals have the required activity needed for the removal of the pollutants during the very short residence times, (2) they are the only catalytic materials with the requisite resistance to poisoning by the residual amounts of sulphur oxide in the exhaust, and (3) they are less prone to deactivation by high-temperature interaction with the substrate oxides of Al, Ce, Zr, etc. used in the catalysts (Shelef and McCabe 2000).

The automobile sector is the largest consumer of PGMs, followed by the jewellery sector (Loferski 2008, 2011).The growth in platinum, palladium and rhodium production from 1998 to

2012 is shown in Figure 1.1, in which it can be seen that in 2012 20% of Pt and 27% of Pd produced were used in the manufacture catalytic converters. The corresponding figure of 36% of Pt and 37% of Pd produced were used in all sectors (Johnson Matthey Platinum 2008, 2013).

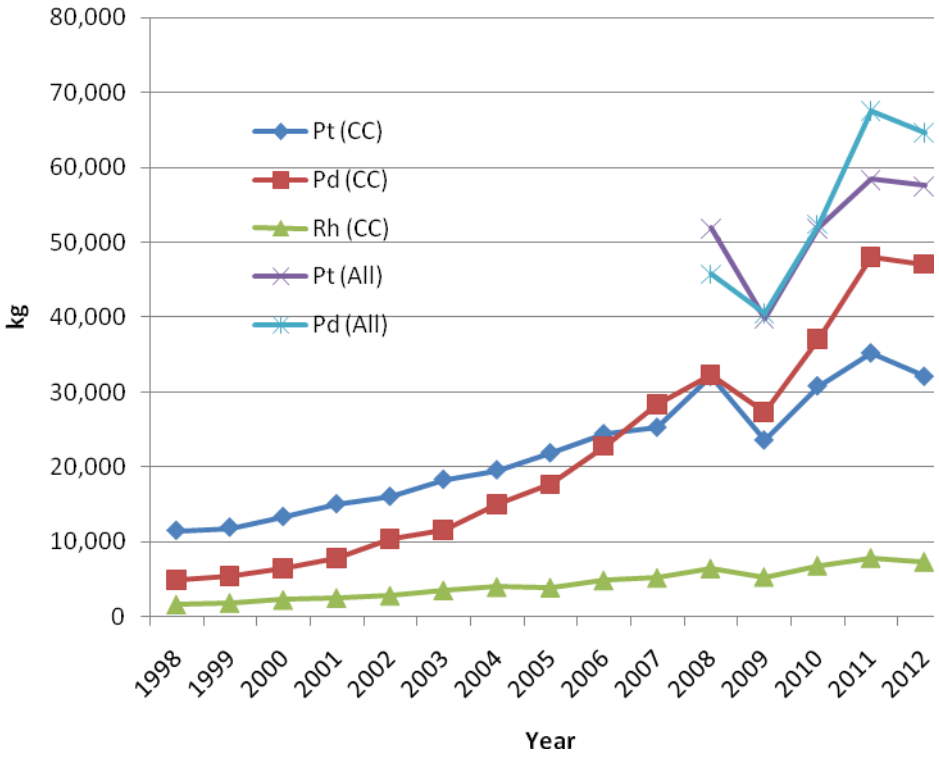

All = catalytic converter (CC) + Electrical + Jewellery

Figure 1.1: Growth in production and application of Pt, Pd and Rh (1998 to 2012)

Source: Johnson Matthey Platinum 2008, 2013

1.3 Problem statement

The natural resources of the platinum group metals are limited and mainly found in Russia, North America, Canada and South Africa. The latter is the world's largest producer of platinum, which is mined in an area known as the Bushveld Igneous Complex.

PGMs occur naturally only at very low concentrations in the earth's crust with a Pt abundance estimated at about 0.005 ppm (Goldschmidt 1954). There is, therefore, considerable interest in reclaiming platinum and other PGMs from scrap components, utilizing a large number of techniques, normally requiring the platinum to be dissolved in suitable lixiviants.

While a great number of technologies have been developed and applied successfully in the reclamation of platinum scrap from spent catalysts (including autocatalysts) there remain a number of challenges. Pyrometallurgical processes are highly energy-consuming and are also highly polluting. Hydrometallurgical processes have become more common, but some of the lixiviants used are composed of dangerous chemicals at high concentrations and some require high reaction temperatures, while corrosion of equipment and the release of dangerous gases such as chlorine and nitrosyl chloride pose serious environmental problems (Jha 2013).

From the above discussion the main practical problem can be identified as a need for a commercially viable hydrometallurgical process for the reclamation of platinum from spent autocatalysts that does not require concentrated and dangerous chemicals or high temperatures, and that causes minimal environmental pollution. A lixiviant therefore needs to be identified that operates under ambient conditions resulting in high PGM recoveries with a minimal impact on the environment.

The main research problem is centred on the electrochemical behaviour of platinum in the mixture of aluminium chloride and nitric acid. The rationale for the choice of the common chloride $AlCl_3$ is that it provides three chloride ions per molecules (while HCl and many of its salts provide only one chloride ion per molecule), approaching the ionic ratio in aqua regia, and the further advantage that leaching solutions with Al^{3+} ions present decrease the dissolution rate of the autocatalyst alumina-containing substrate.

The investigation required certain research questions to be answered.

1.4 Research questions

From an initial literature review it was found that many authors have studied HCl/HNO_3 leaching systems in which a part of the HCl had been replaced by common non-volatile salts, such as NaCl, KCl, $CaCl_2$ and $MgCl_2$. The binary $AlCl_3/HNO_3$ system, however, has not received much attention from researchers (Jha 2013). Based on the foregoing discussion, the following main research question was formulated:

1.4.1 The main research question

The main research question to be answered is, which electrochemical reactions can be identified in an electrochemical study of Pt in different mixtures of aluminium chloride and nitric acid at different temperatures, concentration and pH using a three-electrode electrochemical

cell, and how can these reactions be characterised with a view to possible eventual application in the recovery of platinum from spent automobile exhaust catalysts?

The answering of two minor questions relating to two sub-problems was required in order to increase the scope of the electrochemical investigation. Sub-problem 1 relates to the stability regions of Pt complexes as determined by the relevant Pourbaix diagrams (also known as E_h-pH diagrams). Sub-problem 2 relates to platinum leaching experiments (of limited scope) in which a practical autocatalyst will be subjected to $AlCl_3/HNO_3$-containing lixiviants, in order to test their platinum-reclaiming efficiency at different temperatures. The investigation of Sub-problem 2 is of an exploratory nature, which does not aspire to be an extensive and exhaustive research project, and is not intended as a practical application of any information derived from the answers gained in the pursuit of the main research question. An attempt is merely made to substantiate, through the leaching studies, the electrochemical observations made.

1.4.1.1 Research question pertaining to sub-problem 1

What are the theoretically calculated stability regions of Pt chloro-complexes that may be involved when Pt is subjected to electrochemical polarisation in mixtures of aluminium chloride and nitric acid?

1.4.1.2 Research question pertaining to sub-problem 2

What useful quantitative information can be gained with respect to the dissolution of platinum from a practical automotive catalyst at different temperatures in lixiviants containing different concentrations of aluminium chloride and nitric acid?

1.5 Plan of study and research methodology

The research will be carried out by firstly embarking on a review of selected literature in order to ascertain the current state of theoretical and practical knowledge in the field under investigation. This will be followed by a laboratory investigation from which the findings will be summarised, and which will culminate in conclusions and recommendations for further work.

1.5.1 The literature review

With a view to the interpretation and synthesis of published work, information will be collected from primary, as well as secondary sources in order to establish a basis from which the present investigation could be launched.

The following databases will be consulted:

- Scopus
- ScienceDirect
- Web of Science
- SciFinder

1.5.2 The empirical investigation

In order to gain insight into the nature of thermodynamically stable platinum-containing chemical species that could readily form in mixtures of aluminium chloride and nitric acid under particular sets of pH and potential, theoretical E_h-pH diagrams will be constructed using the HSC 6.1 software.

The aim of the electrochemical part of the investigation will be the generation of potentiostatic *log* j/E curves involving a large variety of temperatures and electrolyte compositions comprising mixtures of $AlCl_3$ and HNO_3. These curves are expected to yield a number of pertinent characteristics of the systems. Firstly, the curves will, essentially, contain information about the actions of the different species in solution under anodic and cathodic conditions. The application of the Nernst equation and the use of published electrochemical potentials will be of considerable help in this regard. It should also be possible to detect the formation and/or removal of surface films present on the platinum electrode surface. Secondly, the polarisation curves recorded at different temperatures have the potential to yield important data, provided that the slopes in the Tafel regions of the diagrams can be determined accurately. From the Tafel slopes at different temperatures it will be possible to establish exchange current densities (j_0) for the different systems. Finally, *via* Arrhenius plots of $\ell n\ j_0$ versus the reciprocal of the temperature, activation energies for reactions in the different electrolytes will be obtained.

In the leaching part of the investigation, finely-divided virgin (unused) automotive exhaust material will be leached at temperatures ranging from 25 to 45 °C in the mixtures of aluminium chloride and nitric acid and the percentage recovery determined at predetermined exposure times.

To conclude the investigation, final conclusions will be drawn and recommendations made.

CHAPTER 2: LITERATURE REVIEW

2.1 Specific objectives of the literature review

The specific objectives addressed in the literature review are to gain insight into the current theory and practice regarding the following topics: the use of PGMs in automotive catalytic systems, the reclamation of platinum from spent catalysts, the chemistry and electrochemistry of Pt in media containing chloride ions, the speciation and complexation of Pt in chloride-containing media and general electrochemical theory.

2.2 Application of PGMs in motor vehicle exhaust systems

In order to remove air pollutants produced by motor vehicles, different approaches are being employed. Ninety eight percent of the pollution caused by motor vehicles can be prevented by the use of catalytic converters, also known as autocatalysts or autocats. In the 1970s the US and Japan implemented the use of catalytic converters in their vehicles. (Harabayashi *et al.* 2012; Fornalczyk *et al.* 2009).

2.2.1 PGMs as catalytic converter materials

Hydrocarbons (C_xH_y), carbon monoxide (CO) and nitrogen oxides (NO_x) are the major automobile exhaust pollutants. C_xH_y and CO occur because the combustion efficiency is less than 100% due to incomplete mixing of the gases and the quenching effect of the colder cylinder walls. The very high combustion temperature results in the thermal fixation of the nitrogen to form NO_x. Each of the three platinum group metals (Pt, Pd and Rh) currently employed in catalytic converters have different roles, which depend on the loading of the catalyst. Pt is used for converting C_xH_y and CO to H_2O and CO_2, while Rh is used to reduce NO_x to N_2 and CO_2. Pd can remove all three pollutants, but is not as effective as Pt or Rh (Fornalczyk *et al.* 2009; Lassi 2003; Upadhyay *et al.* 2013).

The following five reactions can occur in the catalytic converter (Kizilaslan *et al.* 2009; Kobel 2010):

Oxidation of carbon monoxide to carbon dioxide:

$$2CO_{(g)} + O_{2(g)} \rightarrow 2CO_{2(g)} \quad (2.1)$$

Oxidation of unburned hydrocarbons to carbon dioxide and water:

$$2C_xH_{y(g)} + (2x + y/2)O_{2(g)} \rightarrow 2xCO_{2(g)} + yH_2O_{(g)} \quad (2.2)$$

Reduction of nitrogen oxides to nitrogen and oxygen:

$$2NO_{x(g)} \rightarrow xO_{2(g)} + N_{2(g)} \quad (2.3)$$

Steam Reforming:

$$C_xH_{y(g)} + xH_2O_{(g)} \rightarrow xCO_{(g)} + (x + y/4)H_{2(g)} \quad (2.4)$$

Water–gas Exchange:

$$CO_{(g)} + H_2O_{(g)} \rightarrow CO_{2(g)} + H_{2(g)} \quad (2.5)$$

For the reactions to occur, a high temperature (>1 500 °C) is required on the catalyst surface.

2.2.2 The design of the three-way catalytic converter

Three-way catalytic converters (TWC) are the most commonly used catalysts in motor vehicles today (Heck and Farrauto 2001). A combination of Pt, Pd and Rh is employed as active materials in the TWC. Currently TWC formulations containing Pt/Rh, Pt/Pd/Rh (trimetal), Pd only and Pd/Rh are all in commercial use. An advanced automotive TWC can convert more than 99% of CO, hydrocarbons and NO_x into CO_2, H_2O and N_2. TWC typically contain 0.08% Pt, 0.04% Pd and 0.005-0.007% Rh (Shelef and McCabe 2000; Fornalczyk *et al.* 2009; Harjanto *et al. 20*06; Hoffmann 1988a). Catalytic converters consist of a substrate coated with the PGM catalyst, as shown in Figure 2.1.

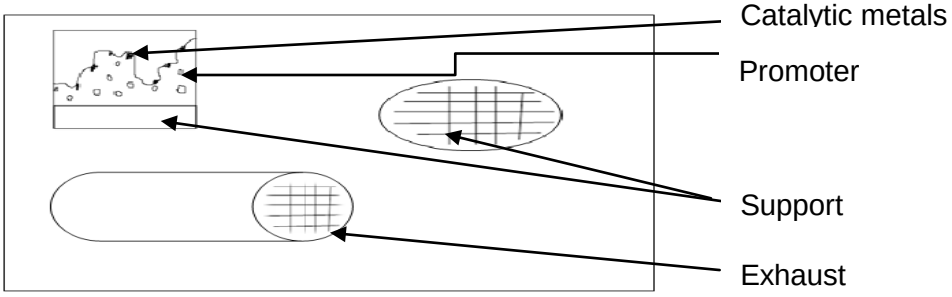

Figure 2.1: Automotive catalysts design

Redrawn from: Lassi 2003

The substrate can either be a ceramic or a metal coated with a support material of aluminium oxide (Al_2O_3) based washcoat, or CeO_2 or ZrO_2. The three-way catalytic converters consist of a ceramic substrate made up of cordierite ($Al_2O_3.2SiO_2.5MgO$) together with PGMs contained in the washcoat. A large active surface area of the catalytic converter is necessary to enhance the catalytic activity. The washcoat layer has a surface area of approximately 50-200 m^2/g, leading to almost 100% conversion due to short diffusion distances thereby ensuring that gases reach the active sites easily. The monoliths are multi-channeled ceramic catalyst bodies (square, triangular or honeycomb channel configurations) with the exhaust gas flowing through the channels (about 1 mm in diameter), the walls of which are coated with a high surface area porous layer of 20 to 60 µm thick, with finely dispersed noble catalytic particles (Shelef and McCabe 2000; Lassi 2003).

The autocatalyst is wrapped and packaged into a stainless steel exhaust structure to form a catalytic converter. The catalytic converter is normally installed as close to the engine as possible. The automobile catalytic converters are generally of three grades in terms of PGM content. Grade 1 consists of 1 200 ppm Pt, 200 ppm Pd and 300 ppm Rh; Grade 2 consists of 1 000 ppm Pt, 200 ppm Pd, and 100 ppm Rh; and Grade 3 consists of 875 ppm Pt, 250 ppm Pd, and 30 ppm Rh (Ravindra *et al.* 2004; Han and Meng 1996).

2.2.3 Leaching of PGMs from spent catalysts

The chemicals and methods commonly used to process spent catalyst metals tend to dissolve even the base matrix holding the PGMs. As a result, existing processes generally suffer from high acid consumption and severe acid corrosion of the processing equipment. New techniques have been developed which are energy-efficient and environmentally acceptable (Han 2007; Upadhyay *et al.* 2013).

In a hydrometallurgical procedure the separation of the PGMs from the catalyst surface is either by means of (a) dissolution of the PGMs, leaving the bulk of the substrate unaffected (Letowski and Distin 1987), or (b) dissolution of the substrate, leaving the PGMs as an insoluble residue. Large amounts of reagents are required by the latter dissolution process and cause severe

waste disposal problems (Angelidis and Skouraki 1996; Bautista *et al.* 1989). This process leaves the PGMs in an insoluble sludge, which requires subsequent dissolution and treatment. From an economic and environmental point of view this procedure is clearly unsatisfactory.

The major challenge in the aqueous extraction of PGMs is the development of a selective leaching system which does not involve the dissolution of the entire catalyst and still achieves high PGM recovery rates. Many authors have investigated the leaching of Pt from spent catalysts with a view to reducing the hydrochloric acid consumption and the generation of gases as found during dissolution with aqua regia. Important parameters to consider for the solubilisation of insoluble materials are temperature, chloride concentrations in the leaching solutions and the effectiveness of oxidants (Letowski and Distin 1987; Letowski and Robinson 1990).

2.3 Leaching methods

Leaching is the extraction of one or more constituents from a heterogeneous solid material by dissolving in a lixiviant solution. Pt extraction from scrap catalytic converters usually involves a 2-step process. The first step is leaching the converter in a solution that transfers Pt incorporated in the converter to an aqueous solution. The second step involves the recovery of pure Pt from this solution. Cyanide and aqua regia are considered good lixiviants due to high percentage recovery, but because of their toxicity some alternative methods are required (Hilson and Monhemius 2005). This section will discuss some traditional as well as newly developed leaching methods.

2.3.1 Cyanide leaching

Cyanide has been used to dissolve platinum group metals from ores at temperature up to 102 C with only limited success owing to low extractions and high cyanide consumption. PGMs and cyanide form soluble complexes in solution. Increasing the leaching temperatures will improve dissolution of the PGM. The PGM-CN complexes which are formed are relatively stable up to decomposition temperatures. A recovery of more than 98% of PGMs has been achieved during leaching using virgin catalysts (Atkinson *et al.* 1989).

Shams *et al.* (2004) have investigated the Pt recovery from a spent industrial dehydrogenation catalyst, using cyanide leaching. The best recovery of 85% Pt was achieved after 1 h with a 2:1 ratio of cyanide to catalyst, a temperature in the range 140 to 180 °C and pH values in the range of 8 to 9. Recoveries of up to 95% Pt were obtained by not basing post cyanide leaching separation on natural sedimentation and decantation, but by employing paper filtration and repeated rinsing for separation of liquid from solids.

Atkinson *et al.* (1989) conducted a study of leaching of virgin automotive catalyst using cyanide. The leaching solution used was 5% sodium cyanide and 1% Ni^{2+} promoter to enhance the reaction at a temperature of 80 °C for 1 h. About 99% of Pd and 98% Pt and as while as for Rh were obtained.

Desmond *et al.* (1991) studied the same procedure using two catalysts: virgin and used catalysts. A slightly different result was observed by doubling the temperature of the above study to 160 °C. For virgin catalyst 97% Pt and 90% Rh were recovered. From used catalysts recoveries of 88, 80 and 75% of Pt, Pd and Rh, respectively, were obtained. The difference in recovery was found to be due to carbon contamination and physical and chemical changes to the catalyst during operation, such as sintering and reaction with the washcoat.

The cyanidation process was studied by Chen and Huang (2006), cited by Jha (2013) to recover PGMs from spent automotive catalysts containing 818.3 g/t Pt, 516.7 g/t Pd and 213.8 g/t Rh. The leaching was slow at room temperature and atmospheric pressure. At elevated temperatures and pressures a cyanide leaching order of Pt>Pd>Rh was found, according to the bond strengths of their complexes.

Huang *et al.* (2006) recovered Pt along with Pd and Rh from spent automotive catalysts by pressure alkaline treatment followed by cyanide leaching. They found that at the PGMs were liberated from their substrates under high-temperature and pressure treatment with NaOH. The pretreated material was then ground for subsequent leaching in cyanide solution. The best metal recoveries were 96% Pt, 98% Pd and 92% Rh. In the cyanide dissolution of PGMs, they found that the reaction rate was controlled by a surface chemical reaction mechanism.

2.3.2 Thiosulphate, thiocyanate and thiourea leaching

The literature search on leaching of the platinum group metals using thiosulphate ($S_2O_3^{2-}$), thiourea (NH_2CSNH_2), and thiocyanate (SCN^-) from automotive catalysts has shown the application of these techniques to be limited. These lixiviants were used as alternatives to cyanide leaching, as cyanide is a toxic pollutant. Xie *et al.* (1996) reported the leaching behaviour of Pd in thiourea (TU) acid solutions. Pd seems to be soluble in solutions containing thiourea, acid and ferric ion. It reacts with ferric ion and thiourea with the overall reaction as follows:

$$Pd_{(s)} + 2TU_{(aq)} + 2Fe^{3+}_{(aq)} \rightarrow Pd(TU)^{2+}_{(aq)} + 2Fe^{2+}_{(aq)} \quad (2.6)$$

The hydrolysis of ferric ion and decomposition of TU was prevented by using a low pH. A high percentage dissolution of Pd was achieved with 0.10 M TU, 0.5 M H_2SO_4 and 0.01 M Fe^{3+} at a temperature of 35 °C with stirring at 500 rpm. An activation energy of about 25.3 kJ/mol in the temperature range of 5 to 35 °C was found, which was believed to indicate chemical reaction control for the dissolution of Pd in thiourea.

2.3.3 Aqua Regia leaching

Aqua regia is a mixture of concentrated hydrochloric acid and nitric acid, in the proportion of 3:1. Pt extraction from used catalysts by aqua regia solution has been studied by numerous investigators (Jafarifar *et al. 20*05, Baghalha *et al. 20*09; Oh *et al.* 2003; Bautista *et al.* 1989). Barakat and Mahmoud (2004) leached spent Pt catalyst gauze dust material containing 13.7% Pt and 1.3% Rh by refluxing with aqua regia at a liquid to solids ratio of 7.5 for 1.5 h to solubilise Pt, which was then separated using trioctylamine and recovered by precipitation. 97.5% Pt recovery was achieved.

Although the Pt extraction rate is very high and fast in aqua regia solutions, the recovery process is challenging (Zanjani and Baghalha 2009). To promote solubility in the acid medium, a strong oxidizing agent is also required to oxidize the precious metal. Oxidizing agents include HNO_3, Cl_2, chlorates, bromides, bromates, iodides, iodates and H_2O_2. HNO_3 is preferred due to the hydrogen ions it can provide, which are necessary to maintain the acidity of the leaching solution (Distin and Letowski 1984). Hydrochloric acid is used as a source of chlorides and for

the required acidity, whereas nitric acid is used as an oxidant (Sheng and Etsell 2007; Aprahamian and Demopoulos 1995; Letowski and Robinson 1990; Bautista *et al.* 1989).

Large amounts of gaseous NO_x and HCl vapours are generated during leaching with aqua regia above 70 °C. The replacing of a part of HCl with other complexing agent sources, such as non-volatile chloride salts, will benefit qua regia (Letowski and Distin 1987).

PGM dissolution in aqua regia involves the formation of chlorine (Cl_2) and (NOCl). Both act as the complexing agents by providing a high oxidation potential and a high chloride ion concentration. It is believed that aqua regia undergoes the following reactions (Baghalha *et al.* 2009; de Aberasturi *et al.* 2011):

$$HNO_{3(\ell)} + 4HCl_{(aq)} \rightleftharpoons NOCl_{(g)} + Cl_{2(g)} + HCl_{(\ell)} + 2H_2O_{(\ell)} \quad (2.7)$$

$$NOCl_{(g)} + H_2O_{(\ell)} \rightleftharpoons HNO_{2(\ell)} + HCl_{(\ell)} \quad (2.8)$$

As a result of reaction (2.7) aqua regia solution is diluted with water, and chlorine and nitrosyl chloride mix to form hydrochloric acid and nitrous acid, as shown above (Sheng and Etsell 2007). A complete dissolution reaction of Pt, Pd and Rh can be obtained in aqua regia as follows (de Aberasturi *et al.* 2011):

$$3Pt_{(s)} + 4HNO_{3(aq)} + 18HCl_{(aq)} \rightleftharpoons 3[PtCl_6]^{2-}_{(aq)} + 6H^+_{(aq)} + 4NO_{(g)} + 8H_2O_{(\ell)} \quad (2.9)$$

$$3Pd_{(s)} + 2HNO_{3(aq)} + 12HCl_{(aq)} \rightleftharpoons 3[PdCl_4]^{2-}_{(aq)} + 6H^+_{(aq)} + 2NO_{(g)} + 4H_2O_{(\ell)} \quad (2.10)$$

$$2Rh_{(s)} + 2HNO_{3(aq)} + 12HCl_{(aq)} \rightleftharpoons 2[RhCl_6]^{3-}_{(aq)} + 6H^+_{(aq)} + 2NO_{(g)} + 4H_2O_{(\ell)} \quad (2.11)$$

In another study conducted by Jafarifar *et al.* (2005) microwave-assisted leaching for the recovery of Pt from spent catalyst was examined. The implementation of microwave-assisted leaching was used to improve the yield of extracted metal and to reduce process time, especially for an environmentally friendly process. They employed two leaching methods: For the first method, the sample was refluxed in aqua regia for 2.5 h with a liquid/solid ratio of 5 at 109 °C. A maximum dissolution yield of 96.5% was achieved. Using microwave heating with a liquid/solid ratio of 2 for 5 minutes, the yield of Pt increased to 98.3%.

Barakat and Mahmoud (2004) examined the recovery of Pt from spent catalyst dust by refluxing, using aqua regia at a temperature of 109 °C for 1.5 h and liquid/solid ratio of 10. The recovery of Pt was 98%.

Oh *et al.* (2003) investigated the recovery of valuable metals (e.g. palladium) from waste printed circuit boards. Pd was leached from the residue using aqua regia at room temperature for 3 h. Pd recovery was speculated to be around 99.9%.

Bautista *et al.* (1989) employed the use of packed and fluidised beds to recover Pt from spent automobile catalysts with aqua regia solution. From a packed bed, recoveries of 96% Pd and 73% Pt were obtained with 3.65 M HCl and 0.35 M HNO_3. The concentration of the mixture was decreased to 3 M HCl and 1 M HNO_3 and the process resulted in 76% Pd and 98% Pt recovery. For the fluidised bed reaction, HCl was substituted with $HClO_4$. A recovery of 93% Pt and 78% Pd was obtained with a 3 M $HClO_4$ and 1 M HNO_3.

Bolinski and Distin (1991) investigated the recovery of Pt and Rh from scrapped autocatalysts by chloride leaching. A solution comprising 8.0 M HCl and 3.5 M HNO_3 can extract about 95% of Pt and 82% of Rh from scrapped honeycomb autocatalysts containing about 950 ppm Pt and 50 ppm Rh. The leach solution was in contact for 3 h at a temperature of about 100 °C.

The high temperatures of above 70 °C make leaching with aqua regia difficult because of environmental concerns. Increased leaching time due to a slow rate of metal dissolution promotes the alumina substrate dissolution of the catalyst, resulting in additional acid consumption (Distin and Letowski 1984).

2.3.4 Halide leaching

Among the various chloride-based lixiviants, hypochlorite is considered to be the most widely used as the oxidizing agent because of its high oxidizing potential (Gupta and Mukherjee 1990; Baghalha 2007; Puvvada and Murthy 2000) conducted a study using chloride/ hypochlorite

solutions to leach precious metals. NaOCl was employed as a lixiviant in the presence of NaCl and HCl. The reaction can be illustrated by equation (2.12) below:

$$NaOCl_{(aq)} + 2HCl_{(aq)} \rightleftharpoons NaCl_{(aq)} + Cl_{2(g)} + H_2O_{(\ell)} \quad (2.12)$$

Harjanto *et al.* (2006) conducted a study of the leaching of Pt, Pd and Rh from automotive catalyst residues in various chloride-based solutions using a mixture of 3 vol% NaOCl and 5 mol/ℓ HCl with the addition of 1 vol% H_2O_2. The leaching time was 3 h at a temperature of 65 °C. Recovery percentages of 88%, 99% and 77% of Pt, Pd and Rh were obtained, respectively.

De Sá Pinheiro *et al.* (2004) studied the recovery of Pt from spent catalytic converters in a fluoride-containing medium at mild experimental conditions after oxidation in a furnace in air. The calcined mass was leached in the presence of HCl and fluoride ions, but was unsuccessful. However, the dissolution of Pt was attained in the presence of strong inorganic acids, and the support material dissolved in 2–4 h at 60 °C. Further studies carried out in the presence of hydrogen peroxide improved the leaching time to less than 1 h. The study showed the possibility of replacing the HNO_3 in aqua regia with hydrogen peroxide. Pt dissolution may be represented by the equation:

$$H_2O_{2(aq)} + 2H^+_{(aq)} + 2e^- \rightleftharpoons 2H_2O_{(\ell)} \quad (2.13)$$

$$Pt_{(s)} + 2H_2O_{2(aq)} + 4HCl_{(aq)} \rightleftharpoons PtCl_{4(aq)} + 4H_2O_{(\ell)} \quad (2.14)$$

$$Pt_{(s)} + 6HCl_{(aq)} + 2H_2O_{(\ell)} \rightleftharpoons [PtCl_6]^{2-}{}_{(aq)} + 2H^+_{(aq)} + 4H_2O_{(\ell)} \quad (2.15)$$

The oxidation and reductions in this system are presented by the following equations given below (Jha *et al.* 2013):

$$Pt_{(s)} + 6I^-_{(aq)} \rightleftharpoons [PtI_2]^{6-}{}_{(aq)} \quad (2.16)$$

$$I_3^-{}_{(aq)} + 2e^- \rightleftharpoons 3I^-_{(aq)} \quad (2.17)$$

Although leaching with iodide/iodine solutions seems to hold promise, very little research has been reported on this system.

Zanjani and Baghalha (2009) investigated Pt extraction from spent reforming catalysts in iodine solution at temperatures from 25 to 95 °C. Finely dispersed Pt was situated on the walls of the nanopores of the gamma alumina support. With regard to the Pt leaching the authors found that particle sizes smaller than 106 µm necessitated vigorous agitation with an impeller speed of 700 rpm to eliminate the effects of catalyst size. The leaching of Pt was controlled by the surface reaction. The solution pH and the concentration of active iodine species were mostly affected by the initial iodine concentration and the liquid to solids ratio. This in turn affected the rate of Pt extraction. Increased concentrations of HCl and a higher temperature also produced faster Pt extraction kinetics. The aluminium of the catalyst support was also partially leached due to the acid present in the lixiviant. After successful validation on a larger scale this process could prove to have potential.

Using a novel method Dragulovic *et al.* (2008) crushed, ground and leached scrap automotive catalysts in hydrochloric acid with nitric acid as oxidant. This treatment produced a chloride solution of the Pt group metals, while the Al_2O_3 catalyst substrate remained undissolved. Cementation of the leached platinum group metals from solution was performed by the addition of powered aluminium at suitable pH values. The precipitate obtained by cementation was a mixture of platinum group metals and surplus aluminium. The surplus aluminium could be removed by treatment with hydrochloric acid. Separation of the platinum group metals was done by conventional chemical processes. It is unlikely that this technique will prove to be economically viable, especially in view of the price of aluminium.

2.3.5 Aluminium chloride leaching

As reported in the literature some authors studied the substitution of part of the HCl in aqua regia type solutions for PGM leaching by a non-acidic solution containing a chloride compound (see previous section). The substituent should be non-volatile and soluble, without crystallising under leaching conditions. The reduced hydrogen chloride evolved during leaching decreases acid consumption (Distin and Letowski 1984; Marinho *et al.* 2010; Zanjani and Baghalha 2009;

Angelidis and Skouraki 1996). A number of suitable non-acidic chloride-containing solutions were identified as potentially effective leaching agents, namely $AlCl_3$, $MgCl_2$, $CaCl_2$, NaCl, and KCl. Chloride ion concentrations of above 12 M can be achieved during the leaching process by these highly soluble salts. Of all the chlorides, $AlCl_3$ is preferred since it provides three chloride ions per molecule. Leaching solutions with aluminium ions present decrease the alumina substrate dissolution rate (Letowski and Robinson 1990; Angelidis and Skouraki 1996).

Letowski and Distin (1985) conducted a study on uncrushed pellets of spent catalysts from which Pt and Pd were leached. A mixture of 0.96 M HNO_3, 2.46 M HCl and 1.46 M $AlCl_3$ was employed. The best yields achieved were 98% for Pt and 97% for Pd.

Letowski and Distin (1987) improved on their 1985 study, by increasing the concentration of chloride to 6.84 M in 0.70 M HNO_3, followed by leaching for 1.5 h at 90 °C. About 90% and 92% of Pt and Pd were recovered, respectively. Increased recoveries of Pt and Pd were obtained during the final washing of the leached bed with $AlCl_3$ solution for 2 h as it cooled down to room temperature and 98 and 97% of Pt and Pd were respectively obtained.

Bolinski and Distin (1991, 1992) also worked on the applicability of an $AlCl_3$ leach process to a honeycomb catalyst to improve Rh recovery by replacing part of the HCl content with $AlCl_3$ to obtain a leachant containing 3.3 M HCl, 0.29 M $AlCl_3$ and 3.5 M HNO_3. The substitution also reduced gas evolution. Complete recovery could be obtained only by physically removing the residual washcoat on leach residue surfaces using a water jet.

The 1992 study by the above-mentioned authors was undertaken to improve the yield by increasing the aluminium chloride concentration. In the first approach a relatively dilute mixture of about 2.0 M HCl and 0.48 M $AlCl_3$ was employed. About 95% of Pt and 82% of Rh were extracted from scrapped honeycomb autocatalysts containing about 1 000 ppm Pt and 50 ppm Rh when leached for 3 h. In the second approach, the solution containing 8.0 M HCl and 3.5 M $AlCl_3$ was boiled. The $AlCl_3$ was added continuously in amounts up to 0.80 M. Increased extraction rates were obtained at temperatures between 120 °C and 160 °C.

Tyson and Bautista (1987) cited in a review article by Furimsky (1996), studied the kinetics of the leaching of Pt and Pd from spent automobile catalysts using a mixture of HCl and HNO_3. A honeycomb form of the catalyst was crushed to obtain 60 to 100 mesh particles. The apparatus comprised a continuous stirred tank reactor (CSTR) in series with a packed bed reactor containing the catalyst and from which the electrolyte was pumped back to the CSTR. The pH and nitrate ion concentration were determined at regular intervals and samples taken for determination of the Pt and Pd concentrations. The maximum leaching time was 25 h. It was found that the kinetics could best be described by the expression

$$C = A \ln (1 + Bt)$$

where C is the concentration of Pt or Pd

t = time in minutes and A and B are constants.

The equation satisfied two boundary conditions, i.e. $C = 0$ and $dC/dt \rightarrow 0$ as $t \rightarrow \infty$. The concentration of Cl^- and NO^-_3 ions influenced the relative rate of leaching of Pt and Pd. When the Cl^- concentration increased and that of NO^-_3 decreased, the extent of Pd dissolution increased and that of Pt decreased, which indicated differences in the mechanism of dissolution of Pt and Pd.

Benke and Gnot (2002) studied the electrochemical dissolution of platinum using cyclic voltammetry, potentiostatic and galvanostatic techniques, and alternating current methods in seven solutions of different HCl concentration varying from 5% to 35%, as well as solutions of KOH (10% and 25%) and H_2SO_4 (10% and 30%). The HCl studies showed that stoichiometric dissolution of platinum was only possible at very low current densities and high HCl concentrations in the electrolyte according to:

$$Pt_{(s)} + 6Cl^-_{(aq)} \rightleftharpoons [PtCl_6]^{2-}_{(aq)} + 4e^- \qquad (2.18)$$

However, the rate of the reaction was too low for practical purposes. The authors found that the use of a sinusoidal alternating current of 50 Hz frequency had a good chance to be successfully

applied in industry. The concentration of HCl in the electrolyte had to be between 25 to 30% and the temperature of the electrolyte between 40 and 45 °C. The current density was chosen within the range from a few thousand to almost 20 000 A m^{-2}. The viability of the method was proven by the dissolution of solid platinum metal, which is normally difficult. The dissolution of Pt sponges and powders would also be possible using this technique.

2.3.6 Summary

In this section the research of a number of researchers has been reviewed in order to obtain a broad overview of aspects which can be expected to feature prominently in a laboratory investigation of the recovery of Pt from scrap autocatalysts.

Pyrometallurgical processes are highly energy-consuming and environmentally unfriendly and the predominant techniques considered are rather based on hydrometallurgical principles.

Hydrometallurgical procedures can be based on either dissolution of the PGMs in appropriate mixtures of chemicals or the dissolution of the substrate, leaving the PGMs as an insoluble residue. The latter method is considered unsatisfactory from an environmental viewpoint.

Lixiviants such as cyanide and aqua regia have found some use. Aqua regia is successful as a lixiviant, but although the Pt leaching rate is high, the economy of the process needs further improvement with regard to the dissolution of the alumina matrix of the catalyst, environmental impact and toxicity. It has, therefore, largely been replaced by mixtures that contain chlorides as complexing agents and nitric acid as oxidant. Alternative methods are also being considered, such as the use of thiosulphate, thiocyanate, and other halides as complexing agents.

The volatility of hydrochloric acid led to the consideration of different metal chlorides as sources of chloride ions, with nitric acid the oxidant and also providing the acidity. Of all the chlorides $AlCl_3$ seems to be preferred since it provides three chloride ions per molecule.

2.4 The general chemistry of Pt

Pt chemistry displays mostly the same features for the different members in the PGMs, but differences are found in stabilities of different oxidation states, stereochemistries, etc.

PGMs cannot exist in oxidation states below zero and their oxidation states are normally between +2 and +8. The reactivity of the PGMs depends on the oxidation states of the metal and the nature of the reactant ligands (Bernadis *et al.* 2005).

2.4.1 Selected chemical properties of Pt

Pt is considered the least reactive metal compared to the other elements in the group, as shown by its relative superior resistance to acids. Pt can occur as Pt^{2+} and Pt^{4+}. Pt^{4+} is the most common ion and its occurrence and properties are discussed by Rao and Reddi (2000) and Hartley (1991). Pt^{4+} is considered thermodynamically and kinetically the most stable ions. Pt belong to the transition metal sub-group with valence electrons in the 5d orbitals. Pt can be complexed by a variety of different ligands. Halide ions can be used as the complexing ligand for Pt. Pt^{4+} when complexed, forms six–coordinated compounds with octahedral structures. Pt has preferences according to their ligand selectivity and coordination compound symmetry of thier properties (Bernadis *et al.* 2005; Greenwood and Earnshaw 1984; Hartley 1991; Gwicana 2007).

2.4.2 The electrochemistry of Pt in chloride/ nitric acid systems

In general, PGMs are very resistant to acid dissolution. Chloro-complexes (e.g. $[PtCl_6]^{2-}$) are formed during the solubilisation of Pt metal with aqueous chloride solutions. This implies that for the formation of Pt chloro-complexes in chloride solution the reduction potential should be greater than 0.74 V for the required oxidising agent (Mishra 1988). The half-reactions with the corresponding standard electrode potentials are as shown in equation as follows:

$$[PtCl_6]^{2-}_{(aq)} + 4e^- \rightleftharpoons Pt_{(s)} + 6Cl^-_{(aq)} \qquad E^o = 0.74\ V \qquad (2.18)$$

Nitric acid is considered a good candidate for solubilising Pt, provided the kinetics of these reactions are favourable (de Aberasturi *et al.* 2011). The reduction reaction of nitric acid is as follows (CRC Handbook 2011-2012):

$$NO_3^-{}_{(aq)} + 3H^+_{(aq)} + 2e^- \rightleftharpoons HNO_{2(aq)} + H_2O_{(\ell)} \qquad E^o = 0.94\ V \qquad (2.19)$$

$$NO_3^-{}_{(aq)} + 4H^+_{(aq)} + 3e^- \rightleftharpoons NO_{(g)} + 2H_2O_{(\ell)} \qquad E^o = 0.96\ V \qquad (2.20)$$

$$2NO_{3\,(aq)}^{-} + 8H_{(aq)}^{+} + 2e^{-} \rightleftharpoons N_2O_{2(g)} + 4H_2O_{(\ell)} \qquad E^o = 0.81\ V \qquad (2.21)$$

These potentials are high enough for the oxidation reaction to occur (Tyson and Bautista 1987). When selecting an oxidant the following have to be considered: (1) the reaction rate, (2) the additional cost of the metal extraction and (3) the difficulties of the downstream processing with nitric acid (Hoffmann 1988b).

For a variety of metals, nitric acid can provide a cathodic process. High current densities can be achieved, hence metal dissolution is fast. Therefore, nitric acid is regarded as an important oxidising acid. Initially nitrate ions are reduced to nitrite. The nitrite reduction probably proceeds through the unstable intermediate nitrous acid (HNO_2) (West 1965).

The nitrous acid can be destroyed to nitric oxide

$$2NO_{2\,(aq)}^{-} + 2\,H_{(aq)}^{+} + 2e^{-} \rightleftharpoons 2HNO_{2(\ell)} \qquad (2.22)$$

$$2HNO_{2(aq)} + 4H_{(aq)}^{+} + 4e^{-} \rightleftharpoons (HNO)_{2(aq)} + 2H_2O_{(\ell)} \qquad (2.23)$$

$$HNO_{3(aq)} + 3H_{(aq)}^{+} + 3e^{-} \rightleftharpoons NO_{(g)} + 2H_2O_{(\ell)} \qquad (2.24)$$

Alternatively nitrous acid may be destroyed by the decomposition

$$2HNO_{2(aq)} \rightleftharpoons NO_{(g)} + NO_{2(g)} + H_2O_{(\ell)} \qquad (2.25)$$

$$NO_{2(g)} + H_{(aq)}^{+} + e^{-} \rightleftharpoons HNO_{2(aq)} \qquad (2.26)$$

$$HNO_{2(aq)} + HNO_{3(aq)} \rightleftharpoons 2NO_{2(g)} + H_2O_{(\ell)} \qquad (2.27)$$

$$2NO_{2(g)} + 2H_{(aq)}^{+} + 2e^{-} \rightleftharpoons 2HNO_{2(aq)} \qquad (2.28)$$

The adding of equations (2.25) – (2.28) results in equation (2.29):

$$HNO_{3(aq)} + 3H^{+}_{(aq)} + 3e^{-} \rightleftharpoons NO_{(g)} + 2H_2O_{(\ell)} \quad (2.29)$$

Priyantha and Malavipathirana (1996) studied the effect of chloride ions on the electrochemical behavior of Pt surfaces by employing the cyclic voltammetric technique. In acid solutions containing chloride ions they found a platinum-containing complex of unknown stoichiometry that could be reduced at a potential 0.5 V more positive than that required for the reduction of surface Pt oxide. In anodic oxidation studies Littauer and Shreir (1966) wrote that most published work agree that the formation of an oxide film (PtO) and/or a Pt-Cl layer precedes the eventual evolution of chlorine at the anode. There seems to be a competition between nitrate and chloride ions for sites on the Pt surface, but the nature of the reactions taking place in this region are unknown. As the potential of the anode is increased the further formation of oxide is overcome and chlorine can eventually evolve at a potential in excess of the normal potential of 1.23 V (SHE). It is therefore clear that the study of the interfacial electrochemistry of Pt is complicated by the formation of various complexes.

2.4.3 The chloro-complexes of PGMs in chloride media

For the solubilisation of Pt from catalysts as chloro-complexes in aqueous chloride, the standard electrode potentials for the half reactions shown in 2.8-2.10 have to be considered. E_h-pH diagrams indicate the thermodynamic requirements of the process and confirm the possible dissolution of Pt as chloro-complexes in HNO_3/ HCl media.

When HCl is used as a stabiliser of the chloro-complexes in the presence of the different oxidizing agents, the oxidation reactions of the PGMs are similar. For the PGM system at low pH and in the presence of NO_3^- in the solution, the redox potential of the solution is close to 1.0 V (SHE). In hydrochloric acid media the corresponding chloro-complexes of the metals are formed (de Aberasturi *et al.* 2011).

De Aberasturi *et al.* (2011), Baghalha *et al.* (2009), Mahmoud (2003) and Harjanto *et al.* (2006) studied the construction of Pourbaix diagrams using various metal and chloride concentrations within a temperature range of 25 to 100 °C. The major metal complex species of $[PtCl_6]^{2-}$, $[PdCl_4]^{2-}$ and $[RhCl_6]^{3-}$ appeared to be stable over a wide range.

Harjanto *et al.* (2006) investigated the E_h-pH diagrams of the Pt-Cl-H_2O, Pd-Cl-H_2O and Rh-Cl-H_2O systems. Pt, Pd and Rh ions appeared as chloro-complexes in the water stability regions while $[RhCl_6]^{2-}$ appeared to occupy a wider range compared to $[PtCl_6]^{2-}$ or $[PdCl_4]^{2-}$. The stability regions of the soluble chloro-complexes of Pt and Pd were limited due to the occurrence of Pd hydroxide and an oxide-hydrate of Pt.

Elding (1970) studied the stepwise dissociation of the tetrachloroplatinate(II) ion in aqueous solutions by separating stable complexes using cation exchange columns and determining and calculating the equilibrium constants, as defined by equation 2.30, from spectrophotometric measurements:

$$K_n = [PtCl_{n-1}(H_2O)_{5-n}^{3-n}] \cdot [Cl^-] \cdot [PtCl_n(H_2O)_{3-n}^{2-n}]^{-1},\ n = 1, 2, 3, 4 \qquad (2.30)$$

Employing solubility measurements Azaroual *et al*. (2001) determined stability constants for a number of Pt species. Table 2.1 compares some of the stability constants reported by Elding (1970) and Azaroual *et al*. (2001) from which it is clear that the constants are subject to uncertainty, possibly due to the different experimental techniques employed.

Table 2.1: Estimated stability constants for β_n (n = 1, 2, 3, 4) for the complex formation between Pt^{2+} and Cl^-

Stability constant	25 °C*	25 °C#
β_1	10^5	$10^{6.3}$
β_2	10^9	$10^{13.1}$
β_3	10^{17}	$10^{16.1}$
β_4	10^{19}	$10^{17.7}$

Sources: *Elding 1970, #Azaroual *et al.* 2001

2.4.4 The speciation of platinum in chloride-containing media

The speciation of hydrogen hexachloroplatinate(IV), also known as chloroplatinic acid (CPA), provides insights into the complex speciation of these Pt compounds. The evolution of the understanding of Pt speciation in electrolytes containing water and chloride ions necessarily

followed the continuous development of more accurate and sensitive analytical techniques. The earliest recorded pathway was the one suggested by Miolati and Pendini (1903), cited by Spieker *et al.* (2002). Basing their investigations on electric conductivity measurements, they suggested that ligand exchange reactions could proceed in a stepwise fashion from $[PtCl_6]^{2-}$ to insoluble reddish brown $[Pt(OH)_6]^{2-}$.

Additionally, chloride ligands can be exchanged by hydroxide ions, leading to a decrease in the pH of the solution. In the Miolati series hydrolysis was proposed to occur as follows:

$$[PtCl_{6-n}(OH)_n]^{2-}_{(aq)} + H_2O_{(\ell)} \rightleftharpoons [PtCl_{5-n}(OH)_{n+1}]^{2-}_{(aq)} + H^+_{(aq)} + Cl^-_{(aq)} \quad (2.31)$$

Where n = 0, 1, 2, 3, 4, 5, depending on pH and concentration.

This model has limited value because no equilibrium constants are given.

Using UV-VIS spectroscopy Sillen and Martell (1971) proposed a pathway consisting of two hydrolysis steps in which chloride is replaced by water, as follows:

$$[PtCl_6]^{2-}_{(aq)} + H_2O_{(\ell)} \rightleftharpoons [PtCl_5(H_2O)]^{1-}_{(aq)} + Cl^-_{(aq)} \quad (2.32a)$$

$$[PtCl_5(H_2O)]^{1-}_{(aq)} + H_2O_{(\ell)} \rightleftharpoons [PtCl_4(H_2O)_2]^{0}_{(aq)} + Cl^-_{(aq)} \quad (2.32b)$$

Assuming that the aquo complexes behave as weak acids, which can dissociate rapidly in basic solutions:

$$[PtCl_5(H_2O)]^{1-}_{(aq)} + OH^-_{(aq)} \rightleftharpoons [PtCl_5(OH)]^{2-}_{(aq)} + H_2O_{(\ell)} \quad (2.33a)$$

$$[PtCl_4(H_2O)_2]^{0}_{(aq)} + OH^-_{(aq)} \rightleftharpoons [PtCl_4(OH)(H_2O)]^{1-}_{(aq)} + H_2O_{(\ell)} \quad (2.33b)$$

$$[PtCl_4(OH)(H_2O)]^{1-}_{(aq)} + OH^-_{(aq)} \rightleftharpoons [PtCl_4(OH)_2]^{2-}_{(aq)} + H_2O_{(\ell)} \quad (2.33c)$$

Therefore, if complete dissociation is assumed, the Pt speciation can be represented by Figure 2.2:

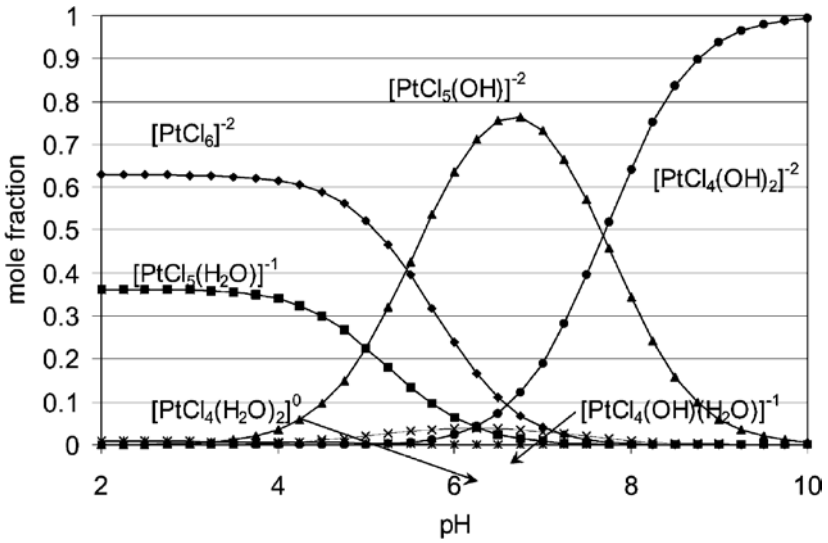

Figure 2.2: Pathways for the speciation of CPA

Source: Spieker *et al.* 2002

Mang *et al.* (1993) cited by Spieker *et al.* (2002) developed a model based on the Sillen and Martell model, but with different dissociation constants.

Lambert *et al.* (1999) studied CPA speciation in the liquid phase using ^{195}Pt NMR. They implemented the same basic pathway as Sillen and Martell (1971). They further reported species such as the cis and trans tetrachloride isomers.

Using Extended X-ray absorption fine structure (EXAFS) Spieker *et al.* (2002) found that the exchange of water molecules with OH ligands was a slow process. The hydroxide-water exchange reaction shown in equation 2.34a further dissociates as shown in equation 2.36b:

$$[PtCl_{6-x}(H_2O)_x]^{-2+x}_{(aq)} + OH^-_{(aq)} \rightleftharpoons [PtCl_x(OH)_y(H_2O)_{x-y}]^{-3+x}_{(aq)} + H_2O_{(\ell)} \quad (2.34a)$$

$$[PtCl_{6-y-z}(OH)_y(H_2O)_z]^{-2+z}_{(aq)} + OH^-_{(aq)} \rightleftharpoons [PtCl_{6-y-z}(OH)_{y+1}(H_2O)_{z-1}]^{-3+z}_{(aq)} + H_2O_{(\ell)} \quad (2.34b)$$

According to the results of Spieker *et al.* (2002) there seems to be agreement with the work done by Miolati and Pendini (1903) cited by Spieker *et al.* (2002) namely that at very low concentration (~30 ppm Pt) a reddish-browish precipitate forms, confirming the presence of six Pt-O bonds. Increasing the concentration of Pt decreases the pH, while PtCl coordination

increases. However, dilute CPA goes through extensive hydrolysis. Table 2.2 provides a summary of chloroplatinic acid (CPA) concentration on pH and EXAFS coordination numbers.

Table 2.2: Effect of CPA concentration on pH and EXAFS coordination numbers

Pt concentration (ppm)	pH measured	Pt-Cl coordination number	Pt-O coordination number
200	2.67	2.8	3.2
500	2.29	3.8	2.2
1000	2.01	4.0	2.0
1500	1.92	4.5	1.5
2000	1.75	4.8	1.2

Source: Spieker et al. 2002

Shelimov *et al.* (2000) used ^{195}Pt NMR and other spectroscopic techniques to study the mechanisms of chloroplatinate adsorption onto alumina. According to the authors Pt species of hexachloroplatinic acid in solution are almost completely dissociated to $[PtCl_6]^{2-}$. This complex anion can undergo two different types of reactions, namely hydrolysis (or aquation–substitution of the original chloride ligands by the H_2O solvent molecules):

$$[PtCl_6]^{2-}_{(aq)} + H_2O_{(\ell)} \rightleftharpoons [PtCl_5(H_2O)]^-_{(aq)} + Cl^-_{(aq)} \quad (2.35)$$

$$[PtCl_5(H_2O)]^-_{(aq)} + H_2O_{(\ell)} \rightleftharpoons [PtCl_4(H_2O)_2]_{(aq)} + Cl^-_{(aq)} \quad (2.36)$$

The possibility of these reactions occurring, is generally recognized, according to Shelimov *et al.* (2000). Theoretically, it is possible that the process could continue, providing more deeply hydrolyzed Pt complexes. Further aquations are, in fact, only observed when the temperature is increased, and in basic solutions. Reactions (2.35) and (2.36) are ligand substitutions on an inert low-spin d^6 complex and, therefore, very slow. The authors state that quantitative evaluation is hampered by the rather different values that have been reported for the respective equilibrium constants. They estimate log K_4 to be about -1.7.

2.4.5 Summary

In summary it can be stated that the evolution of the theory of Pt speciation has seen a long development from a relatively rudimentary scheme to a much more complicated picture in which the initial reaction (aquo ligand exchange of chloride ions) is rapid and also reversible, while subsequent reactions, namely hydroxide ion ligand exchange of chloride and aquo ligands are relatively slow. High chloride-containing complexes are more stable in acid solutions and high chloride concentrations, resulting in $[PtCl_6]^{2-}$ as the main species under these conditions.

2.5. Fundamental electrochemical theory

2.5.1 Introduction

In this section, anticipating the major role of electrochemistry expected to be played in the experimental part of this investigation, a brief overview of the relevant electrochemical theory was presented, starting with the Butler-Volmer equation. The Butler-Volmer equation, by rearrangement, leads to the Tafel equation from which two crucial electrochemical parameters can be derived, namely the Tafel slopes of the cathodic and anodic polarisation curves. The intersection of the polarisation curves facilitates the determination of the exchange current density, which can be used to calculate the activation energy of electrode reactions occurring near the equilibrium electrode potential.

The activation energies provide indirect evidence of the nature of the reactions occurring at the metal surface near the equilibrium electrode potential e.g. whether they are of a chemical (reaction) or physical (adsorption) nature. In view of the importance of obtaining accurate Tafel slopes, special attention was given to the problem of determining the “slope” from non-linear polarisation curves. A paper on the application of the Gauss-Newton method, as one possible approach to non-linear curve fitting, was included in the literature study.

Finally, literature on the chemical reactions anticipated in the experimental study was consulted, which highlighted the importance of reactions involving platinum, both during polarisation and during electrode preparation prior to commencement of potentiodynamic scanning. The electrode potentials of seemingly important reactions were collected from various sources.

Electrochemical processes exhibit fundamental parameters that are important in the aqueous dissolution of metals, namely the electrode potential (E_e) (volt) and current density (j) (A cm^{-2}.) The electrochemistry of a corroding metal involves two or more half-cell reactions. In the anodic half-cell reaction oxidation occur allowing electrons to flow to the cathode where reduction takes place (Pletcher 2009; McCafferty 2005).

At the equilibrium of these two reactions (the cathodic and anodic), the rate is balanced and there is no net flow of electrons. Hence $j_0 = 0$ where $j_a = -j_c = j_0$

j_0 is the exchange current density in A cm^{-2}

The electrode potential is given by the Nernst equation:

$$E = E^0 + 2.303\frac{RT}{nF}\log Q \qquad (2.37)$$

The reaction quotient (Q) has the same mathematical form as the equilibrium constant expression (K), i.e. the ratio of the activities of products to the activities of reactants. Q is numerically equal to K only when the reactants and products are in equilibrium (in which case the cell potential, E, will be zero). T is the absolute temperature, F the Faraday constant (96 480 C mol^{-1}) and R the gas constant (equal to 8.3144 J mol^{-1} K^{-1}).

This equation links the electrode potential with the activities of the reactants.

2.5.2 The Butler-Volmer equation

When a net current flows through the electrochemical cell the cell is not in equilibrium, and the half-cell potential will deviate from the equilibrium value by the overpotential:

$$\eta = (E - E_0) \qquad (2.38)$$

If an electron-transfer process consisting of the single elementary step, of which the forward reaction (the cathodic or reduction rate) is first order in O in a stirred electrolyte

$$O + e \rightleftharpoons R$$

is considered, Rieger (1987) shows that the difference between the cathodic and anodic reaction rates is the net flux of O at the electrode surface and thus proportional to the net current, i:

$$j = FA[k_c C_0 - k_a C_R] \quad (2.39)$$

where k_c and k_a are the rate constants for the cathodic and anodic reactions, and C_O and C_R are the respective concentrations.

The rate constants for the cathodic and anodic reactions, respectively, will be given by

$$k_c = k_{c0} \exp \frac{(1-\beta)F\eta}{RT} \quad (2.40)$$

and

$$k_a = k_{a,0} \exp \frac{\beta F \eta}{RT} \quad (2.41)$$

where k_c and k_a are the rate constants for the cathodic and anodic reactions, $k_{c,0}$ and $k_{a,0}$ the rate constants at zero current, β the transfer coefficient, T the absolute temperature, F the Faraday constant (96 480 C mol^{-1}) and R the gas constant (equal to 8.3144 J mol^{-1} K^{-1}) (Rieger 1987).

Substituting equations 2.42 and 2.43 into equation 2.41 and rearranging, leads to the Butler-Volmer equation (B-V E):

$$j = j_o \left\{ \exp\left(\beta \frac{nF}{RT} \eta \right) - \exp\left(1 - \beta \frac{nF}{RT} \eta \right) \right\} \quad (2.42)$$

Where β is the symmetry coefficient and η the overpotential.

Equation (2.42) relates the electrode potential to the net current density. B-V E describes the two reactions (cathodic and anodic), which are assigned as follows: the first term

$j_a = \mathrm{j}_0 \exp(\beta \frac{nF}{RT}\eta)$ is for the anodic reaction and the second $j_c = \mathrm{j}_0 \exp(1-\beta \frac{nF}{RT}\eta)$ describes the cathodic reaction. From these two reactions a graph of η vs log j can be plotted (Trethewey and Chamberlain 1995; Trasatti 2009; McCafferty 2005; Bard and Faulkner 1980).

Over a short potential range the two reactions oppose each other, but become essentially unidirectional when one reaction occurs at a negligible rate.

The B-V E can be rearranged to give the Tafel equation in terms of the logarithm (Bard and Faulkner 1980; ASM 1987:30):

$$\eta_a = b_a \log(\frac{j_a}{j_o}) \tag{2.43}$$

Where b_a is the anodic Tafel coefficient (sometimes indicated as β_a) given by:

$$b_a = \frac{2.303\,\mathrm{RT}}{\beta\eta F} \tag{2.44}$$

Similarly at cathodic overpotentials a Tafel coefficient b_c (sometimes indicated as β_c) can be obtained for the metal cation deposition:

$$b_c = \frac{2.303\,\mathrm{RT}}{(1-\beta)\eta F} \tag{2.45}$$

The Tafel slopes b_a and b_c are powerful electrochemical parameters (Trasatti 2009; Bard and Faulkner 1980; ASM 1987).

The Tafel equation can be expressed in the following (West 1965):

$$\eta = \mathrm{a} \pm \mathrm{b} \ln \mathrm{j} \tag{2.46}$$

From the above it follows that a plot of η against ln j should yield a straight line from which the Tafel slopes b_a and b_c could be determined from the slope of the Tafel lines. The intercepts would yield ln j_0 from which it follows that the rates of the activation reactions occurring at equilibrium are directly proportional to ln j_0. By utilizing the Arrhenius equation, the temperature dependence of the reactions at equilibrium can be determined, thereby making the estimation of the activation energy possible.

2.5.3 Tafel extrapolation method to determine exchange current

The Tafel equation indicates how the exchange current and the transfer coefficient may be determined.

If for an equilibrium mixture of oxidant and reductant, the current is measured as a point of overpotential and then plotted as log j vs .η, a linear region is found. This is the region governed by activation kinetics. If the linear portions of the plot of the anodic and cathodic curves are extrapolated to zero overpotential, the log of the exchange current is given by the intercept and the transfer coefficients by the slopes.

The Tafel equation indicates that the current increases exponentially with increasing overpotential. At some point the current becomes limited by the rate of transport and the log j vs. η plot begins to flatten. This is the point at which concentration overpotential becomes dominant and is dependent on the efficiency of stirring and on the diffusion coefficients (Zaki 2006; ASM 1987; McCafferty 2005; Rieger 1987).

When the cathodic reaction is negligibly small the anodic reaction from the Tafel equation may be written in the following manner:

$$j = j_0 \exp \frac{\beta F \eta}{RT} \tag{2.47}$$

From the equation when using logarithm it follows that

$$\log j = \log j_0 + \frac{\beta F \eta}{2.3 RT} \tag{2.48}$$

For β = 0.5, R = 8.314 J mol^{-1} K^{-1} and F = 96 500 C mol^{-1} the following equation is obtained:

$$\log j_0 = \log j + 2520\frac{\eta}{T} \quad (2.49)$$

2.5.4 Evans and polarisation diagrams

The term Evans diagram originated in electrochemical corrosion studies to refer to a diagram in which electrical potential is plotted, as the independent variable on the vertical axis, and generated electrical current as the dependent variable on the horizontal axis. The intersection between the curves gives the corrosion potential E_{corr}, which is measured in volts. The current density and j_{corr} is usually reported in amperes per square centimeters (A/cm^2.) (Breuer and Jeffrey 2002; West 1980; Zaki 2006).

The Evans diagram differs from the polarisation curve as it displays the reaction rates in current densities (j) whereas polarisation curve data display externally applied current densities (j_{app}) (Kelly *et al.* 2002).

Polarisation diagrams are widely used in the electrochemical field, such as shown in Figure 2.3 for a single electrode potentiostatically polarised in the positive and negative directions in an electrolyte.

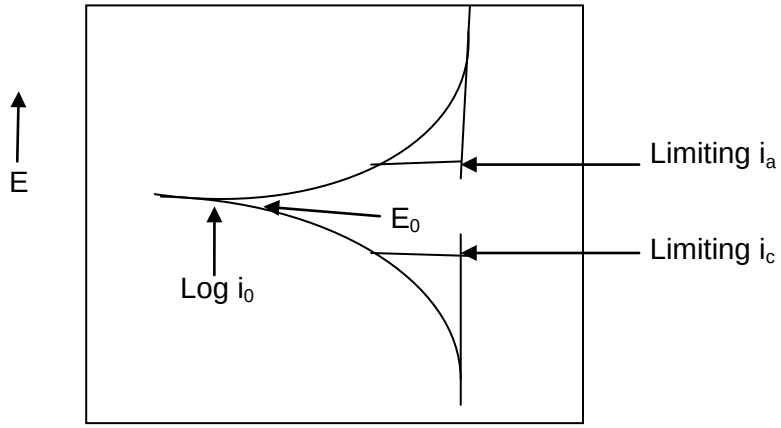

Figure 2.3: Polarisation diagram showing limiting anodic and cathodic current densities and both activation and concentration overpotentials

Redrawn from: West 1965

2.5.5 Determining the slopes of Tafel lines

Tafel slopes of polarisation curves are important parameters for the determination of useful data, such as the exchange current density and activation energy of electrochemical reactions.

Kear and Walsh (2005) remarked that, although frequently misused the Tafel slope in chemical systems is a very useful parameter and needs proper consideration.

From linear polarisation curves, Tafel slopes can be determined and poses no challenges for the requirement of the existence of pure activation control is ensured. Non-linear polarisation curves have two difficulties:

- When the control changes from pure charge transfer to mass control it is not possible to obtain Tafel slopes
- Attempting to obtain Tafel slopes is complicated by the problem of establishing the appropriate potential at which the determination has to be carried out. In most cases a tangent is taken at a small potential for example 10 mV. A somewhat better approach is to determine slopes at several points within a range of potentials and calculate the average slope. This approach was followed by Ravera and Chavez (2005) and is explained in Figure 2.4. They proposed a numerical calculation method using the Gauss-Newton algorithm (based on the Butler-Volmer equation). The method entails the use of experimental values of overpotentials and current densities to generate optimised Tafel curves, allowing the calculation of the average of the slopes at all the data points in the potential region of choice.

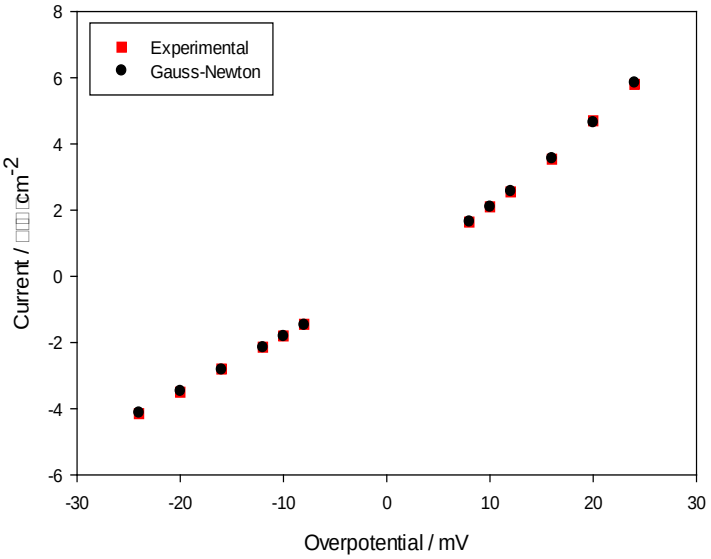

Figure 2.4: Polarisation curve using the Gauss-Newton method

Redrawn from: Ravera and Chavez 2005

2.5.6 Arrhenius plot

According to the Arrhenius equation the rate of a chemical reaction is given by the following equation:

$$Rate = A\exp\frac{-E_a}{RT} \tag{2.50}$$

with A the constant, E_a the activation energy, R the gas constant and T the absolute temperature.

Linearising the Arrhenius equation leads to the following:

$$\ln Rate = \ln A - \frac{E_a}{RT} \tag{2.51}$$

From equation (2.51) it is clear that if ln rate is plotted against 1/T, a straight line should be obtained. The slope of the line and the y intercept give $-E_a/R$ and ln A, respectively (Atkins 2006).

2.6 Thermodynamic studies

In hydrometallurgical processes thermodynamic investigations are considered most important to employ in order to shed light on the stability of different species in an aqueous solution. For calculating thermodynamic parameters and data compilation, powerful software packages are available, e.g *Phase Equilibria Database, FACTSage, STABCAL, and HSC Chemistry*. (de Aberasturi *et al.* 2011; Baghalha *et al.* 2009; Mahmoud 2003; Angelidis and Skouraki 1996). The software packages facilitate the fast construction of thermodynamic diagrams at the temperatures, pressures and concentrations of interest.

The predominant stability areas can be obtained as a function of pH and electrochemical potential (E_h), and are known as Pourbaix or E_h-pH diagrams. Limitations of E_h-pH diagrams include: no information provided on reaction kinetics, the diagrams are derived for specific temperature and pressure conditions and the diagrams are derived for selected concentration of ionic species (HSC Chemistry® 6.1 manual 2006; Osseo-Asare *et al*. 2010).

2.6.1 Summary

Powerful software packages and data bases are available for the theoretical computation of stability diagrams, such as E_h/pH (Pourbaix) diagrams. While these diagrams have inherent limitations in that, for example, they do not provide kinetic data, and have limitations with regard to concentrations of species, temperatures and pressures, they are helpful in visualising stability regions under specific conditions of E_h and pH. A number of researchers has been reviewed in order to obtain a broad understanding of Pourbaix construction and reveals the different stability regions on PGMs which can be expected when plotting the Pourbaix diagrams.

Angelidis and Skouraki (1996) reported the Pourbaix diagram of the system platinum-water at 25 °C with a solution of chloride concentration of 1 M and Pt concentration of 10^{-4}. In the presence of excess chloride anions, the Pt chloride complexes were stable at pH values below 1, to preventing hydrolysis and adsorption on the undissolved substrate. The tetrachloride complex seemed to be unstable in aqueous solutions.

In Chapter 3 the experimental methods and materials employed in this investigation will be described.

CHAPTER 3: EXPERIMENTAL

3.1 Introduction

This chapter describes the experimental approaches in the investigation of the dissolution of platinum metal employing leaching and electrochemical techniques, using mixtures of aluminium chloride and nitric acid as lixiviants and supporting electrolytes at various temperatures and concentrations.

The E_h-pH module of the thermodynamic software HSC Chemistry 6.1 developed by Rione and Anttila (2006) was used to map out possible stable phases in the aqueous electrochemical systems involving platinum, platinum chloro-complexes and platinum oxides. For the electrochemical investigation a potentiostat with Power Suite software was employed.

3.2 Materials and their preparation

3.2.1 Chemical reagents

All chemical reagents were obtained from Associated Chemical Enterprises (ACE) and were of analytical grade (AR). Nitric acid ($HNO_{3(\ell)}$) of 55% concentration and a density of 1.34 kg/ℓ was used in the experiments as an oxidizing reagent. Aluminium chloride (99% $AlCl_3.6H_2O_{(s)}$) was used as the complexing agent for the system. Demineralised water from a Millipore Milli-Q Plus ultra-pure water system was used for solution preparation and for dilution. When required, nitrogen gas ($N_{2(g)}$) provided by Afrox Ltd was bubbled through solutions for 10 minutes to remove the oxygen.

3.2.2 Preparation of solutions

Nitric acid was prepared as a stock solution in a 1 000 mℓ volumetric flask and was further used to prepare the various concentrations for the study. Aluminium chloride was weighed off according to the concentrations required. All solutions were prepared in 500 mℓ volumetric flasks.

3.2.3 The autocatalyst investigated

Finely ground (-1 mm) virgin automotive catalytic converter material was supplied by Johnson Matthey (Pty) Ltd. The material composition is proprietary, but the platinum loading was divulged to the researcher for the purposes of this investigation. Results are therefore given as percentages Pt recovered, and not in terms of weight of Pt recovered.

3.3 Apparatus and procedures

3.3.1 Construction of Pourbaix diagrams of oxides and chloro-complexes of Pt

In this study the construction of E_h-pH diagrams was considered to be a prerequisite for electrochemical and leaching investigations. The diagrams were required to shed light on the stability regions of Pt-complexes.

HSC Chemistry 6.1 software of Rione and Anttila (2006) was used to construct the Pourbaix diagrams. Before Pourbaix diagrams could be constructed the formation constants of the different Pt species were required. From the formation constants the Gibbs free energy of formation (ΔG_f^o) of each complex can be calculated. The HSC database was found to be incomplete and, therefore, the IUPAC Database of Stability Constants and NIST Database for Critically Selected Stability Constants (NIST 8.0 2004) were searched for stability constants for complexes of Pt, with Cl^-, as well as OH^-.

Table 3.1 below displays the stability constants and Gibbs energies of formation of ligand complexes for chlorides and hydroxides of Pt. Table 3.2 contains thermodynamic data for some cations and anions.

Table 3.1: Stability constants and Gibbs energies for Pt with ligands of interest				
Ligand	**Formula**	**log β**	**ΔG^o kJ/mol**	**ΔG_f^o kJ/mol**
Cl^-	$[ML]/[M].[L]$	5.00	-28.50	-57.86*
	$[ML_2]/[M].[L]^2$	9.00	-51.38	-211.99*
	$[ML_3]/[M].[L]^3$	11.80	-67.36	-412.24*
	$[ML_4]/[M].[L]^4$	13.80	-78.78	-545.52*
	$[ML_6]/[M].[L]^6$	-24.70	141.01	-755.58#
OH^-	$[ML]/[M].[L]$	24.42	-139.34	-92.96^
	$[ML_2]/[M].[L]^2$	29.25	-166.89	-344.50^

M = Metal, L = Ligand.

Source: *Elding 1970; #Whitfield 1974; ^Nabivanets *et. al*. 1970

Table 3.2: Thermodynamic data for the individual cations and anions		
Ion	**H_f^o, kJ/mol**	**S_f^o, kJ/mol**
Pt^{2+}	243.55	-9.0000×10^{-02}
Cl^-	-167.08	5.6735×10^{-02}
OH^-	-230.02	-2.0240×10^{-02}

Source: CRC Handbook of Physics and Chemistry 2011-2012

The Gibbs free energy (ΔG^0) for each complex can be calculated by the following equation:

$$\Delta G^0 = 2.303\, RT \log \beta \qquad (3.1)$$

where R is the universal gas constant, T is the absolute temperature and β is the formation constant of a specific complex.

For individual cations and anions the standard free energy of formation can be calculated by using equation (3.2) and the values of the relevant enthalpies and entropies shown in Table 3.2.

$$\Delta G_f^0 = \Delta H_f^0 - T\Delta S_f^0 \quad (3.2)$$

The standard Gibbs free energy of formation of complexes can be calculated as follows:

$$\Delta G_f^0 = \Sigma \Delta G_{f\,products}^0 - \Sigma \Delta G_{f\,reactants}^0 \quad (3.3)$$

Sample calculations of free energies of formation are given in Appendix A.

3.3.2 Electrochemical procedure

Electrochemical experiments were carried out in a three-electrode electrochemical cell comprising a working, reference and counter electrode. The schematic diagram of the electrochemical setup is depicted in Figure 3.1. A working electrode (0.196 cm^2 area, obtained from Pine Instruments) was used as a stationary disc electrode. The counter electrode was platinum foil (area about 2 cm^2). The reference electrode used, was an Ag/AgCl electrode. All potentials measured were converted to the standard hydrogen electrode (SHE) scale. The working electrode was carefully polished with gamma alumina paste of 1.0 µm particle size, followed by 0.05 µm. After polishing, the electrode was rinsed with demineralised water, dipped into a beaker with demineralised water for a few minutes, rinsed again with water and wiped dry with a paper towel before being used. These steps were repeated before every scan.

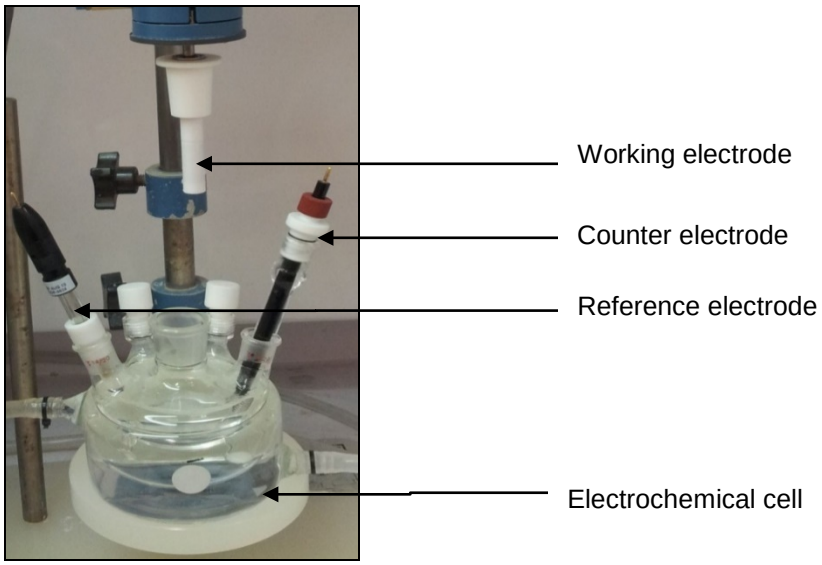

Figure 3.1: The electrochemical setup

All electrochemical investigations were conducted in a water-jacketed cell at temperatures of 25, 35, and 45 °C, with the temperature regulated by means of a Julabo F12 ED thermoregulator (water bath). The three electrodes contacted the solution through sockets in the lid of the electrochemical cell. The solution compositions are shown in Table 4.1. The electrodes were connected to the potentiostat using alligator clips, as shown in Figure 3.2. Care was taken to keep the solution away from the electrical connections. All linear polarisation (LP) experiments were carried out by employing a scan rate of 10 mV/s from the equilibrium potential, either in the anodic or cathodic direction.

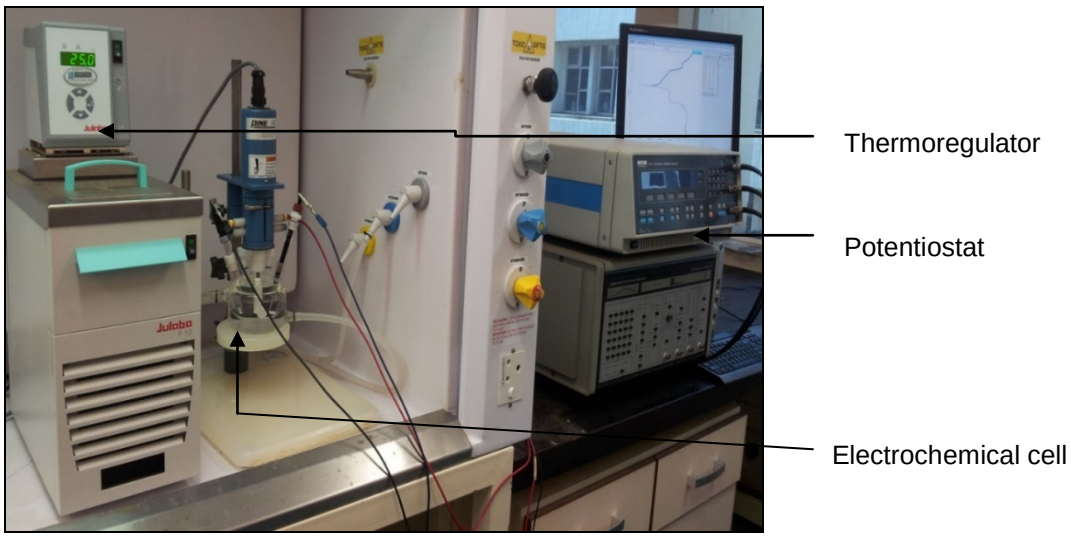

Figure 3.2: The electrochemical investigation setup

3.3.3 Treatment of polarisation data

Polarisation curves of η vs. log j were obtained for a large number of combinations of electrolytes and temperatures and subsequently analysed with the aid of available data from the literature.

In order to arrive at values of j_0, slopes of the different polarisation curves were taken at a point 50 mV removed from the equilibrium potential E_e in either direction. This point was chosen arbitrary, except that care was taken to establish that was inside the activation region of the polarisation curves. From the values of the slopes obtained (b_a and b_c – the Tafel slopes for the anodic and cathodic polarisation curves, respectively) the points of intersection could be calculated, yielding values of j_0.

In order to somewhat address arbitrariness of the choice of the points to determine the slopes, the polarisation data (overpotential η and log j) from each polarisation (some 2 000 individual data points per run) were captured and read into Excel spreadsheets. The object was to derive the b_a and b_c values as well as the exchange current j_0 density. For this purpose the simplified Tafel equation was employed:

$$\eta = a \pm b \ln j \qquad (3.4)$$

The value of j_o is included in the intercept, as explained in Section 2.6.1.

By performing linear regression analyses on the η and log j data, slope and intercept data could be obtained readily. The range used in the regression analysis was restricted to the overpotential range 0.01 to 0.1 mV. In this way it was hoped to restrict the determination of the slope and intercept to the region of activation overpotential. The success of this strategy would show up in a high value of the correlation coefficient, thereby indicating the absence of concentration overpotential (mass transfer) which would cause strong deviation from linearity.

3.3.4 Leaching procedure

The three solutions selected to be tested in leaching experiments are shown in Table 3.3.

Table 3.3: Electrolytes used for the leaching experiments	
Designation	**Composition $AlCl_3$+HNO_3**
A	0.015 M + 0.1 M
F	0.2 M + 0.3 M
I	0.6 M + 0.9 M

A simple schematic diagram of the experimental setup is shown in Figure 3.3. The apparatus consisted of a 500 mℓ round bottom flask as the leaching vessel, situated in the heating mantle. The thermometer, stirrer, Liebig cooler and thermocouple were inserted through the five-necked lid and the fifth opening was covered with a stopper to prevent any loss of gases and solution due to evaporation. The heating mantle and thermocouple, together with the controller with LCD display were used to control the temperature. A piece of aluminium foil was inserted between the flask and heating mantle to facilitate even spreading of the heat.

Solutions of selected concentrations of aluminium chloride and nitric acid were prepared and added to the 500 mℓ round bottom flask. About 15 g of accurately weighed platinum-containing material was added to the solution and mixed together. The solid to liquid ration was therefore about 30 g/ℓ. The solution was then heated and stirred until it reached the desired temperature (25, 35 or 45 °C). Stirring was kept constant at a rotation speed of 300 rpm. All ground glass fittings were sealed, using vacuum grease to ensure tightness, and the Liebig cooler was used to minimise evaporation. The total leaching time was 24 h. Samples (10 mℓ) were taken at 2 h intervals for the first 8 h and at 4 h intervals thereafter.

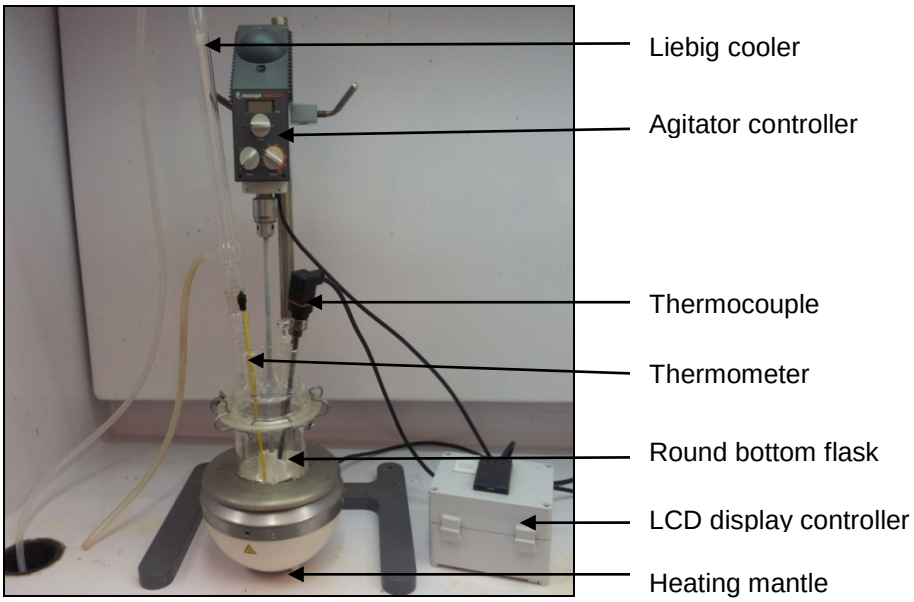

Figure 3.3: The leaching setup

The leaching solution was left to cool to room temperature and was then separated by filtration, using a Büchner funnel as shown in Figure 3.4. The residue was washed with distilled water and the filtrate made up to 100 mℓ in a standard flask. Aliquots were then taken for ICP analysis. A sample calculation of the percentage recovery of Pt is shown in Appendix B.

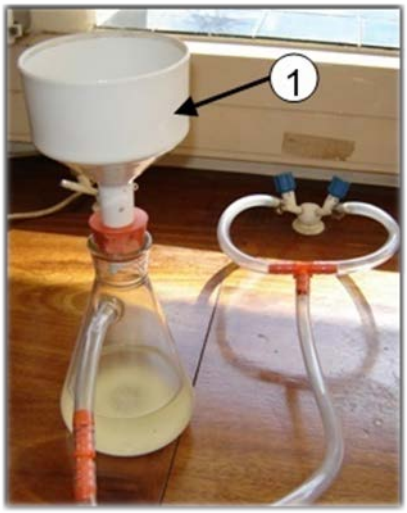

Figure 3.4: A typical filtration setup

3.3.5 Inductively coupled plasma optical emission spectroscopy (ICP-OES)

The solution was taken for analysis in an Inductively Coupled Plasma-Optical Emission Spectrophotometer (iCap 6000 from Thermo Fisher Company), as shown in Figure 3.5. The spectroscopic technique was used for determining the percentage of the platinum recovered during the leaching process. The calibration curve for the determination of Pt with the ICP is shown in Appendix C.

Figure 3.5: ICP-OES instrument

CHAPTER 4: RESULTS AND DISCUSSION

4.1 Introduction

This chapter focuses on the results obtained from the study of the dissolution of platinum, focusing on thermodynamic, electrochemical and leaching investigations employing the experimental procedures discussed in Chapter 3. The aim is to gather information relevant to the reclaiming of platinum from spent automotive catalytic converters. A list of the electrolytes employed in this investigation is given in Table 4.1. The investigations were carried out at temperatures of 25, 35 and 45 $^{\circ}$C.

Table 4.1: Electrolyte Designation

Designation	Composition $AlCl_3$+HNO_3
A	0.015 M+0.1 M
B	0.03 M+0.1 M
C	0.06 M+0.1 M
D	0.05 M+0.3 M
E	0.1 M+0.3 M
F	0.2 M+0.3 M
G	0.15 M+0.9 M
H	0.3 M+0.9 M
I	0.6 M+0.9 M

4.2 Construction of pourbaix diagrams

All Pourbaix diagrams were constructed using the HSC Chemistry 6.1 program (Roine and Anttila 2006). The concentration of chloride ions and the temperatures were varied in order to obtain a clear understanding of the Pt-Cl-H_2O system. Diagrams were constructed for electrolytes A, B, C, D, E, F, G, H, I, listed in Table 4.1.

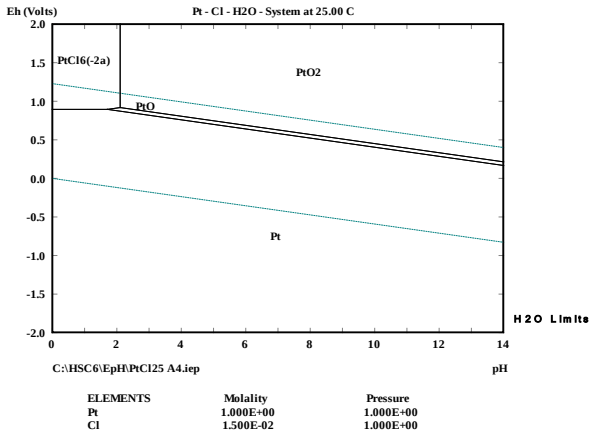

(a)

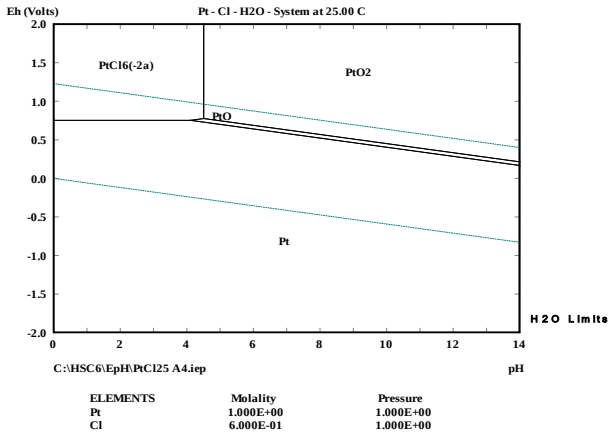

(b)

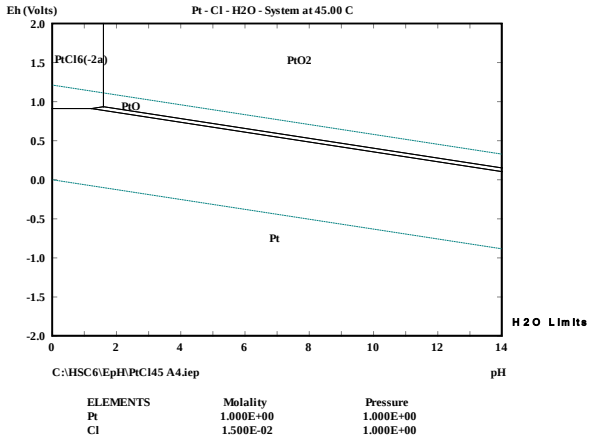

(c)

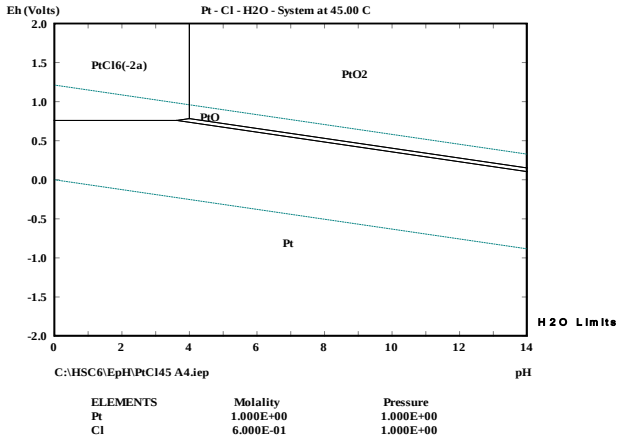

(d)

Figure 4.1: E_h-pH diagram of Pt- Cl- H_2O system for (a) 0.015 M $AlCl_3$ + 0.1 M HNO_3 at 25 $^{\circ}$C (b) 0.6 M $AlCl_3$ + 0.9 M HNO_3 at 25 $^{\circ}$C, (c) 0.015 M $AlCl_3$ + 0.1 M HNO_3 at 45 $^{\circ}$C (d) 0.6 M $AlCl_3$ + 0.9 M HNO_3 at 45 $^{\circ}$C

The E_h-pH diagrams shown in Figure 4.1 are for the selected electrolytes at temperatures of 25 and 45 $^{\circ}$C while the other results are contained in Appendix D. Figures 4.1(a) and (b) depict chloride concentrations of 0.015 and 0.6 M at 25 $^{\circ}$C. Figure 4.1(a) shows that $[PtCl_6]^{2-}$ is stable at around pH 2 and a potential above 1 V. The increase in chloride concentration extends the stability region of the hexachloro complex $[PtCl_6]^{2-}$ to about pH 5.

Comparison of Figures 4.1(a) and (c) shows the effect of increasing the temperature from 25 to 45 °C. It is clear that the stability area of the hexachloro complex is somewhat smaller at the higher temperature, not extending to a pH of about 2. A similar, though less pronounced effect of temperature is seen by comparing Figure 4.1 (b) and (d). It is concluded that higher chloride concentrations and lower temperatures favour the extension of the stability region of the hexachloro Pt complex. PtO_2 stability appears to be lying mostly outside the stability region of water, while PtO is stable in water from the region of chloro-complex stability to pH 14.

4.2.1 Summary

The present work seems to be in agreement with the findings of Angelidis and Skouraki (1996), where the same stability regions of platinum-complexes were observed. The Pourbaix diagrams show that, within the concentration and temperature ranges studied in this research, $[PtCl_6]^{2-}$, PtO_2, PtO need to be considered. These compounds will feature prominently in electrochemical reactions involving platinum, as will be discussed in the next section.

4.3 Electrochemical studies

The results of cathodic and anodic potentiodynamic polarisation curves gave rise to the electrochemical data relating to the behaviour of Pt metal in solutions containing chloride ions and nitric acid, as listed in Table 4.1 above.

4.3.1 Interpretation of potentiodynamic polarisation curves

The polarisation curves were plotted as potential (E in volts, V (SHE)) vs. the logarithm of current density (log j (A cm^{-2}), in accordance with the Tafel equation:

$$\eta_a = a_a + b_a \log j \qquad (4.1)$$

$$\eta_c = a_c - b_c \log j \qquad (4.2)$$

where

η = overpotential (V on the SHE scale)

j = current density (A cm^{-2})

a = constant incorporating the exchange current density (j_0)

b_a and b_c are the Tafel slopes of the anodic and cathodic curves, respectively.

A large number of polarisation curves were obtained under various conditions of composition and electrolyte temperature. As these polarisation curves show almost identical features they are not all included in the discussion. Appendices E and F contain the rest of the polarisation curves. Figures 4.2 to 4.13 shown below are typical examples of the curves obtained and were therefore selected for detailed analysis. In all instances the rate of polarisation was 10 mV/s. The potential was scanned from the equilibrium potential E_e to either -2 V (cathodic) or 2 V (anodic), as required, always starting with a fresh electrode surface in order to ensure that the initial surfaces were film free. Subsequently the two parts of the polarisation diagrams were combined to present a single, comprehensive diagram.

In the following sub-sections attempts will be made to establish which reactions occurred during the anodic and cathodic polarisation runs. Table 4.2 contains anodic and cathodic reactions that were considered relevant in the analyses of the polarisation curves:

Table 4.2: Reduction potentials of relevant electrochemical reactions at 25 °C

Reaction	Potential V (SHE)
$[PtCl_4]^{2-}_{(aq)} + 2e^- \rightarrow Pt_{(s)} + 4Cl^-_{(aq)}$	+0.73*
$[PtCl_6]^{2-}_{(aq)} + 2e^- \rightarrow [PtCl_4]^{2-}_{(aq)} + 2Cl^-_{(aq)}$	+0.74*
$PtO_{2(s)} + 4H^+_{(aq)} + 4e^- \rightarrow Pt_{(s)} + 2H_2O_{(\ell)}$	+1.00
$PtO_{2(s)} + 2H^+_{(aq)} + 2e^- \rightarrow PtO_{(s)} + H_2O_{(\ell)}$	+1.01
$O_{2(aq)} + 4H^+_{(aq)} + 4e^- \rightarrow 2H_2O_{(\ell)}$	+1.23
$Cl_{2(g)} + 2e^- \rightarrow 2Cl^-_{(aq)}$	+1.36
$2H^+_{(aq)} + 2e^- \rightarrow H_{2(g)}$	0.00
$NO_3^-{}_{(aq)} + H_2O_{(\ell)} + 2e^- \rightarrow NO_2^-{}_{(aq)} + 2OH^-_{(aq)}$	-0.01
$O_{2(aq)} + H^+_{(aq)} + 2e^- \rightarrow HO_{2(aq)}$	-0.13#
$2CO_{2(aq)} + H_2O_{(\ell)} + 2e^- \rightarrow H_2C_2O_{4(aq)}$	-0.48#
$2NO_3^-{}_{(aq)} + 2H_2O_{(\ell)} + 2e^- \rightarrow N_2O_{4(aq)} + 4OH^-_{(aq)}$	-0.85

Sources: Handbook of Physics and Chemistry 2011-2012; # Rieger 1987; * Bautista *et al*.1989

4.3.2 Anodic polarisation curves

A summary table of the different polarisation curves obtained experimentally is shown in Appendix G. It can be seen that many of the measurements were repeated, sometimes up to four times in order to establish repeatability, and also with a view to comparing results obtained in different contexts.

Figure 4.2 illustrates an experimental anodic polarisation curve. The curve depicts a scan from the equilibrium potential through the Tafel region and progressing to the final positive potential of +2 V (SHE). At the equilibrium potential the net sum of the anodic and cathodic reaction rates on the electrode surface is zero. A dynamic equilibrium is established, which is depicted by the exchange current density (j_o).

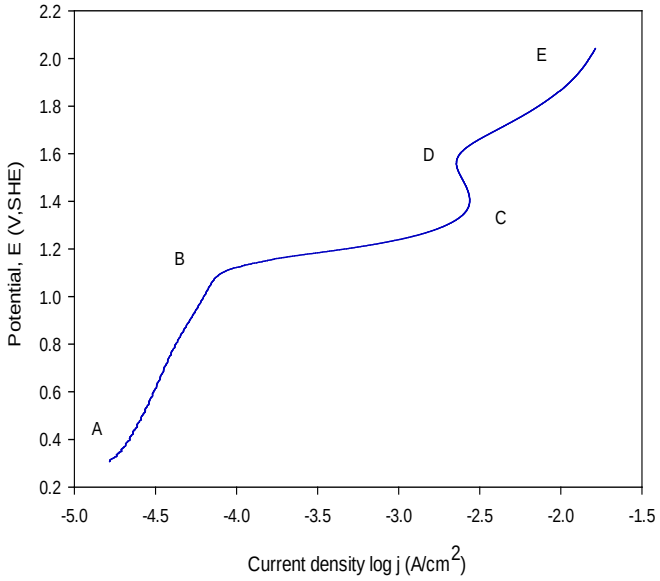

Figure 4.2: Polarisation curve of Pt at 25 °C in 0.05 M $AlCl_3$ and 0.3 M HNO_3 after N_2 deaeration

Within region AB the dominant reactions are probably the progressive physical and chemical adsorption of chloride ions. Li *et al.* (1992) studied surface coverage of chloride ion using the Electrochemical Quartz Crystal Microbalance (QCM) and found that the surface coverage of chloride is 100% between 0.5 and 0.6 V (SHE). Specific adsorption of chloride ions begins right from the equilibrium potential region (Patil *et al.* 2011), until a potential of about 0.73 V is reached, which points to the occurrence of the following reaction (refer to Table 4.2):

$$Pt_{(s)} + 4Cl^-_{(aq)} \rightleftharpoons [PtCl_4]^{2-}_{(aq)} + 2e^- \qquad E^0 = +0.73\ V \qquad (4.3)$$

There is then a gradual conversion of $[PtCl_4]^{2-}$ to $[PtCl_6]^{2-}$, starting at about 0.74 V (SHE). The reactions occurring in the potential region B to C have been subjected to numerous studies, but the issue of whether the oxygen exists on platinum surface in this potential region as chemisorbed species or in the form of oxides has still not been completely resolved (Patil *et al.* 2011). The polarisation curve seems to indicate that the chloride complexes accumulate on the electrode surface, partially passivating the platinum electrode in region BC (possibly with platinum oxides (PtO_x) also present). The influence of stirring the electrolyte on the existence of the chloride film is discussed in Section 4.3.3.

According to Patil *et al.* (2011) the oxide film on Pt grows in two stages in the presence of Cl^- ions. The first stage in film formation is the growth of PtO. At higher potentials the second stage occurs which involves the formation of PtO_2.

In the present work it is suggested that the two-stage formation of PtO_2 takes place as per the following reactions at a potential close to 1.00 V (point B in Figure 4.2):

$$Pt_{(s)} + 2H_2O_{(\ell)} \rightleftharpoons PtO_{2(s)} + 4H^+_{(aq)} + e^- \qquad E^0 = +1.00\ V \qquad (4.4)$$

$$PtO_{(s)} + 2H_2O_{(\ell)} \rightleftharpoons PtO_{2(s)} + 2H^+_{(aq)} + e^- \qquad E^0 = +1.01\ V \qquad (4.5)$$

These oxides will tend to passivate platinum as shown by the slope change at point C. Beyond point C, in the potential range 1.2 to 1.4 V, the current density decreases considerably, indicating the active dissolution of platinum via a growing PtO_2 surface film, which is believed to have a reasonably high ionic conductivity (Patil *et al.* 2011).

Littauer and Shreir (1966) wrote that it is generally agree that the existence of an oxide film (PtO_x) and/or a Pt-Cl layer precedes the eventual anodic evolution of chlorine on Pt. At point D (Figure 4.2) the potential for chlorine evolution is about 1.4 V. This seems to be in agreement with the findings of Littauer and Shreir (1966), who came to the conclusion that, only on

reaching a potential of about 1.36 V, the further formation of oxide can be overcome and chlorine can evolve according to the reaction shown below (see Table 4.2).

$$2Cl^-_{(aq)} \rightleftharpoons Cl_{2(g)} + 2e^- \qquad E^0 = +1.36\ V \qquad (4.6)$$

At point D a change in the slope of the curve occurs at a potential of about 1.9 V, which can be ascribed to oxygen evolution. Oxygen evolution is normally expected at about 1.23 V (see Table 4.2) according to the reaction:

$$2H_2O_{(\ell)} \rightleftharpoons O_{2(g)} + 4H^+_{(aq)} + 4e^- \qquad (4.7)$$

"Delayed" oxygen evolution seems to be a special feature of anodic reactions on the platinum-group metals in aqueous solutions. Patil *et al.* (2011) present data from the literature dealing with possible mechanisms of oxygen evolution on platinum electrodes. It appears that some fourteen different mechanisms have been reported in this regard. Some researchers attempted to distinguish various mechanisms on the basis of the Tafel slopes, and the effect of pH and oxygen partial pressure on the current density.

There seems to be agreement on the role of adsorbed halide ions on the platinum electrode surface. It appears that specifically adsorbed chloride ions compete with oxygen for sites on the Pt surface, thereby retarding oxide film formation. The concentration of water on the surface of the electrode is of crucial importance for the water oxidation reaction shown above. Chloride ions will occupy almost 100% of the surface area, especially if the concentration exceeds about 0.25 M (Patil *et al.* 2011). Water is therefore expelled from the surface and the electrode potential at which water oxidation can commence is increased, as can be seen from the Nernst equation:

$$E = E^o + \left(\frac{\mathrm{RT}}{\mathrm{nF}}\right)\ln\left\{\frac{[O_2]\,[H^+]^4}{[H_2O]^2}\right\} \qquad (2.37)$$

As the concentration of water is lowered the electrode potential is shifted to higher values. The above explanation seems to be consistent with the sudden current increase in region DE found in the present research.

4.3.3 The influence of stirring on anodic curves

Stirring the electrolyte or rotating the electrode will have the effect to enhance the movement of species towards the electrode surface, thereby increasing the rate of the relevant reactions.

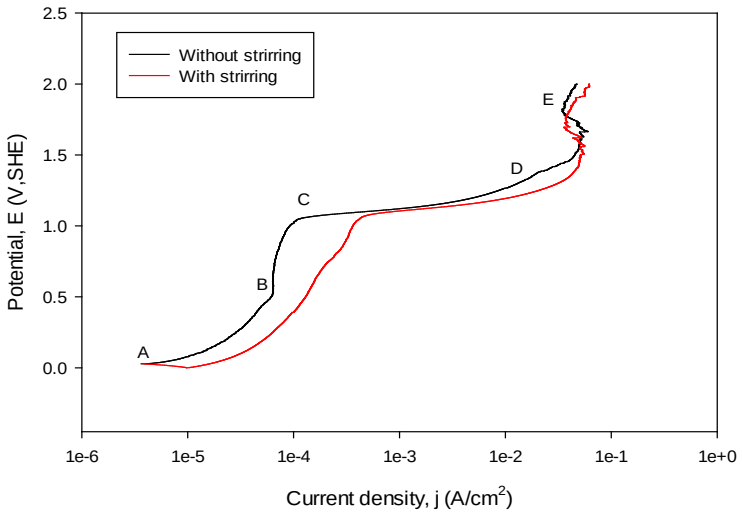

Figure 4.3: The anodic polarisation curve of Pt in 0.6 M $AlCl_3$ and 0.9 M HNO_3 at 25 °C with and without stirring during scanning

With reference to the curves in Figure 4.3 it appears that, whereas a tendency to passivate is observed in the potential region 0.5 to 1.1 V (also refer to Figure 4.2 region BC), this tendency is removed by stirring. This leads to the conclusion that the rate of transport of chloride ions to the Pt surface is rate-determining in this potential region. Stirring therefore enhances the rate of formation of, e.g. $[PtCl_6]^{2-}$, according to the following reaction:

$$[PtCl_4]^{2-}_{(aq)} + 2Cl^-_{(aq)} \rightleftharpoons [PtCl_6]^{2-}_{(aq)} + 2e^- \qquad E^0 = +0.74\ V \qquad (4.8)$$

$[PtCl_6]^{2-}$ probably has a higher solubility in the electrolyte than $[PtCl_4]^{2-}$ and consequently the passivating role of the tetrachloro-complex is lessened, resulting in an increase in the anodic current.

4.3.4 Cathodic polarisation curves

Figure 4.4 illustrates the cathodic polarisation curve obtained by scans from the equilibrium potential E_e (point A) to a potential of -2 V SHE at point E.

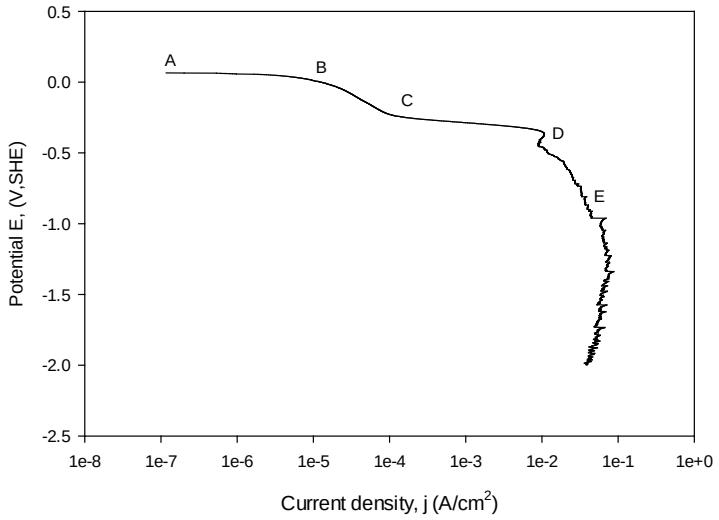

Figure 4.4: The cathodic polarisation curve of Pt in 0.6 M $AlCl_3$ and 0.9 M HNO_3 at 35 ˚C

$$2H^+_{(aq)} + 2e^- \rightleftharpoons H_{2\,(g)} \qquad E^0 = 0.00\ V \qquad (4.9)$$

The overall hydrogen evolution reaction (HER) on metallic surfaces usually occurs in two stages (West 1965; Pletcher 2009).

$$H^+_{(aq)} + e^- \rightarrow H_{ads} \text{ (Volmer reaction)} \qquad (4.10)$$

followed by either

$$2H_{(ads)} \rightarrow H_{2(g)} \text{ (Tafel reaction)} \qquad (4.11)$$

or

$$H^+_{(aq)} + 2H_{(ads)} + e^- \rightarrow H_{2(g)} \text{ (Heyrowski reaction)} \qquad (4.12)$$

where $H_{(ads)}$ indicates hydrogen atoms adsorbed on the metallic surface (also frequently depicted as a M-H bond).

The HER occurs at a very slight activation overpotential in the region. Point B probably indicates the onset of nitrate ion reduction to nitrite by the reaction:

$$NO_{3\,(aq)}^{-} + H_2O_{(\ell)} + 2e^{-} \rightleftharpoons NO_{2\,(aq)}^{-} + 2OH_{(aq)}^{-} \qquad E^0 = -0.01\ V \qquad (4.13)$$

Reaction (4.13) is the initial cathodic nitrate reduction step. At low current densities this reaction is the rate-limiting step (West 1965) and continues from B to C, exhibiting a measure of concentration polarisation with increasing current. The rate-limiting step then possibly passes to the formation of NO from NO^{-}_{2} according to the following reaction:

$$NO_{2\,(aq)}^{-} + H_2O_{(\ell)} + e^{-} \rightarrow NO_{(aq)} + 2OH_{(aq)}^{-} \qquad E^0 = -0.46\ V \qquad (4.14)$$

The limiting of the current at potentials lower than -0.46 V can be ascribed to slow diffusion of NO_2^- ions to the platinum surface. Rotation of the electrode or stirring the electrolyte during polarisation leads to a higher cathodic current (see Figure 4.6, red curve). This reaction is then followed by the reduction of nitrite ions to N_2O_4 ($2NO_2$):

$$2NO_{3\,(aq)}^{-} + 2H_2O_{(\ell)} + 2e^{-} \rightleftharpoons N_2O_{4(g)} + 4OH_{(aq)}^{-} \qquad E^0 = -0.85\ V \qquad (4.15)$$

In region CDE there seems to be many possible reactions to consider, as depicted in Figure 4.5, the investigation of which falls outside the scope of this dissertation. It does however seem possible that gas evolution can occur up to a potential of -2 V.

$$NO_3^- \longrightarrow NO_2 \longrightarrow NO_2^- \longrightarrow NO \longrightarrow N_2$$

Figure 4.5: Possible reactions in the electrochemical reduction of nitrate ions in acid solution Redrawn from Khaled 2010

Finally, point E marks the onset of the cathodic reduction of PtO_2 (possibly formed during sample preparation and initial exposure to the electrolyte). Reduction of PtO_2 to PtO and Pt metal could occur according to the following reactions:

$$PtO_{2(s)} + 4H^+_{(aq)} + 4e^- \rightleftharpoons Pt_{(s)} + 2H_2O \qquad E^0 = -1.00\ V \qquad (4.16)$$

$$PtO_{2(s)} + 2H^+_{(aq)} + 2e^- \rightleftharpoons PtO_{(s)} + H_2O \qquad E^0 = -1.01\ V \qquad (4.17)$$

4.3.5 Influence of stirring on cathodic curves

Stirring of the electrolyte and/or rotating the electrode can be useful in studying reaction mechanisms in electrochemical systems. Figure 4.6 below confirms the occurrence of diffusion-limited reactions by showing a marked shift in the current densities beyond point C on the red curve (corresponding to point D in Figure. 4.4, as discussed in Section 4.3.4). The limiting current observed may be due to concentration polarisation due to a buildup of N_2O_4 gas on the electrode surface.

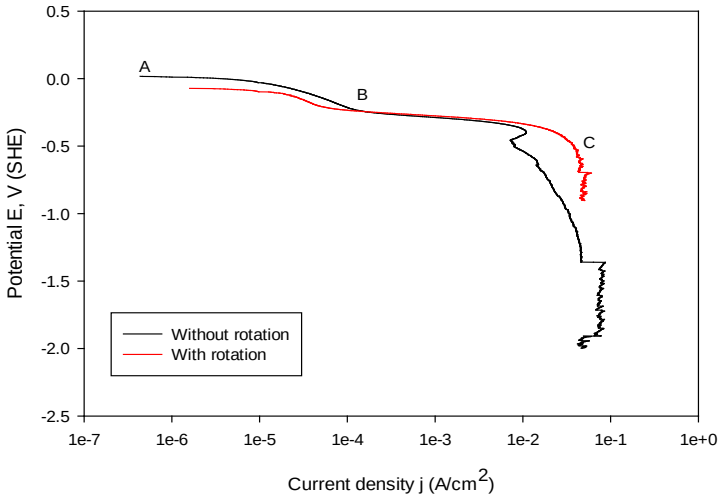

Figure 4.6: The cathodic polarisation curve of Pt in 0.6 M $AlCl_3$ and 0.9 M HNO_3 at 25 °C with and without electrode rotation during scanning

4.4 Composite polarisation curves

The influence of certain parameters become clearer by looking at composite anodic/cathodic polarisation curves.

4.4.1 Influence of nitrogen deaeration on composite polarisation curves

Figures 4.7 and 4.8 reveal that when nitrogen has been bubbled through the solution a slight decrease in the equilibrium potential occurs. The reactions involved in the two figures are similar, except that when nitrogen has been bubbled through the electrolyte before starting the scan, the current does not show the slight slope in the curve between about +0.2 and -0.2 V found in the oxygen-containing electrolyte, as shown in Figure 4.7, recorded at 25 °C.

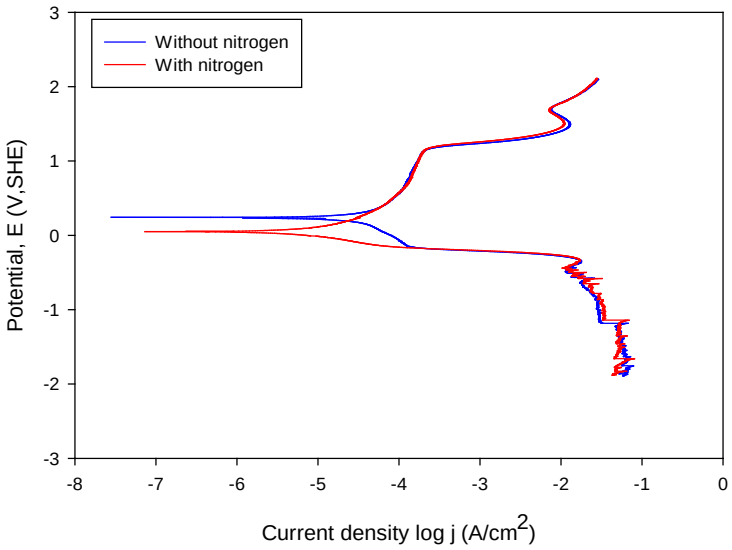

Figure 4.7: Polarisation curve of Pt in 0.15 M $AlCl_3$ and 0.9 M HNO_3 at 25 °C, with and without nitrogen deaeration

Figure 4.8 shows that when the temperature is increased to 45 °C the relative current densities determined in aerated and deaerated electrolytes are not influenced much, although deaeration leads to a slightly more negative Pt equilibrium potential. The current density during N_2O_4 gas evolution is slightly higher when deaeration has been performed prior to polarisation, possibly indicating the absence of inhibiting oxide films.

In Figure 4.8 the sloping curve between +0.2 and -0.2 V is conspicuously absent in the curve obtained without prior nitrogen sparging when compared with the results shown in Figure 4.7 (blue line). It is therefore hypothised that a possible explanation for the sloping curve may be the presence of oxygen in the electrolyte. Electrocatalytic ORR occurs via three pathways: the 1-

electron transfer pathway, producing superoxide ion, the 2-electron transfer pathway, producing hydrogen peroxide; and the 4-electron transfer pathway, producing water (Song and Zhang 2008). The latter pathway is dominant on Pt, but the electrode potential of -1.23 V does not fit the potential curves obtained. The following equation describes the reduction of dissolved oxygen in acid electrolytes to form hydrogen dioxide (Rieger 1987), possibly as an intermediate species in the 4 electron "associative mechanism" described by Song and Zhang (2008), which involves adsorbed oxygen on the Pt electrode.

$$O_{2(aq)} + H^{+}_{(aq)} + e^{-} \rightarrow HO_{2(aq)} \qquad E^{0} = -0.13\ V \qquad (4.18)$$

With regard to the presence and solubility of oxygen in the different electrolytes, reference to Figures 4.9 to 4.13 shows that the possible ingress of oxygen into the electrolytic cell during polarisation or inadequate deaeration before polarisation has to be considered. Reference to Figure 4.13 also highlights the possibility of the lower solubility of oxygen in more concentrated electrolytes. Due to diminished oxygen solubility in the electrolyte at 45 °C, equation 4.18 is prevented.

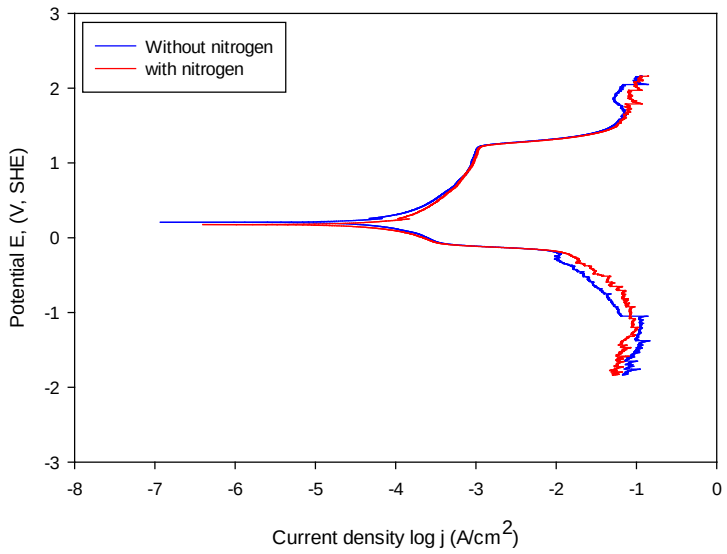

Figure 4.8: Polarisation curve of Pt in 0.2 M $AlCl_3$ and 0.3 M HNO_3 at 45 °C with and without nitrogen deaeration

In order to establish whether the sloping curves observed between +0.2 and -0.2 V can indeed be ascribed to the presence of dissolved oxygen and not to the reduction of nitrogen-containing species, polarisation curves that had been obtained in nitrate-free electrolytes were compared with the present results. In an electrochemical study of the oxidation of Pt in electrolytes

containing only ozone, oxygen and chloride ions Mogwase (2012) found that the sloping curves were present in all the polarisation diagrams recorded. In the present study the hypothesis regarding the sloping curves between +0.2 and -0.2 V is supported by the following results, which relate to the availability of dissolved oxygen in the electrolyte: Figure 4.9 (temperature increased from 25 to 45 °C, leading to reduced solubility of O_2 in the electrolyte), Figure 4.10 (increasing concentrations of $AlCl_3$ resulting in reduced solubility of O_2 in the electrolyte, Figure 4.13 (high concentrations and a high temperature, both leading to reduced solubility of O_2 in the electrolyte).

4.4.2 Influence of temperature on composite polarisation curves

Figure 4.9 shows the polarisation curves of Pt at 25, 35 and 45 °C in 0.03 M $AlCl_3$ and 0.1 M HNO_3, illustrating the effect of temperature on the polarisation curves. More results are contained in Appendix E

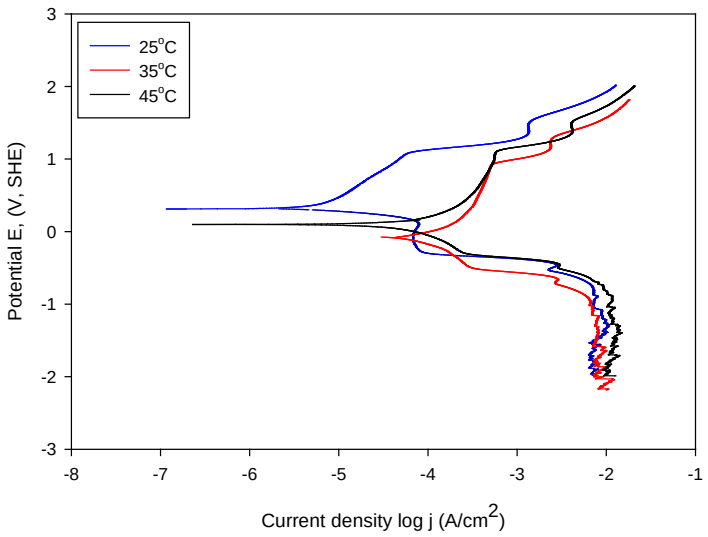

Figure 4.9: Polarisation curves of Pt at 25, 35 and 45 °C in 0.03 M $AlCl_3$ and 0.1 M HNO_3 after nitrogen deaeration

According to the Nernst equation:

$$E = E^0 + 2.303\frac{RT}{nF}\,log\,\frac{[Oxidised\ state]}{[Reduced\ state]} \quad (2.37)$$

an increase in the temperature of the electrolyte will lead to an increase in electrode potential. It can also be expected that the rate of electrode reactions will increase, as shown by a shift of the polarisation curves to higher current densities at 25 °C. However, as the temperature was increased from 25 °C to 35 °C and to 45 °C (Figure 4.9) the relative positions of the polarisation curves did not change as expected. The relative shift to lower anodic currents (compared to the 25 °C curve) when the temperature was increased to 35 °C and 45 °C, can be explained in terms of the competition between oxide film formation on Pt and the formation of a $[PtCl_x]^{2-}$ film on the electrode surface. The shift in the anodic curves to lower current values as the temperature is increased seems to indicate that the chloride complexes (possibly $[PtCl_4]^{2-}$ changing into $[PtCl_6]^{2-}$ with increasing potential) form as continuous films with lower ionic conductivities. This leads to more effective passivation of the platinum electrode. At about 1 V the formation of platinum oxides (e.g. PtO and PtO_2) commence, as discussed earlier in Section 4.3.2.

4.4.3 Influence of chloride ion concentration

Figure 4.10 shows the polarisation curves of Pt in electrolytes with chloride concentrations of 0.015, 0.03, 0.06 M with 0.1 M HNO_3 at 25 °C. Figure 4.11 shows similar results obtained when the temperature was increased to 45 °C, showing that the higher the chloride concentration, the higher the current densities.

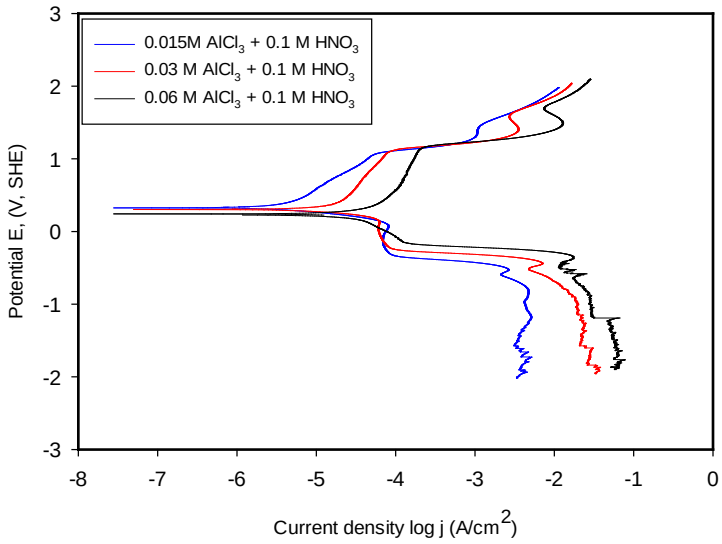

Figure 4.10: Polarisation curves of Pt in 0.015, 0.03 and 0.06 M $AlCl_3$ and 0.1 M HNO_3 at 25 C after nitrogen deaeration

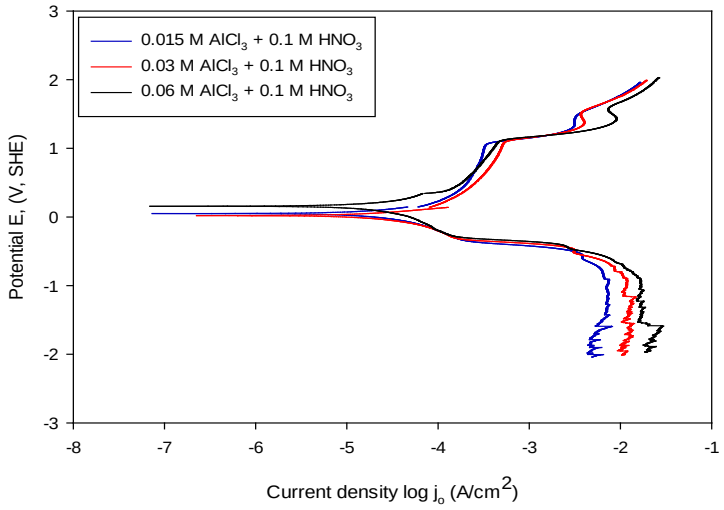

Figure 4.11: Polarisation curves of Pt of 0.015, 0.03 and 0.06 M $AlCl_3$ and 0.1 M HNO_3 at 45 C after nitrogen deaeration

Figures 4.11 to 4.13 illustrate the influence of increasing both the $AlCl_3$ and HNO_3 concentrations on the polarisation curves at a temperature of 45 °C.

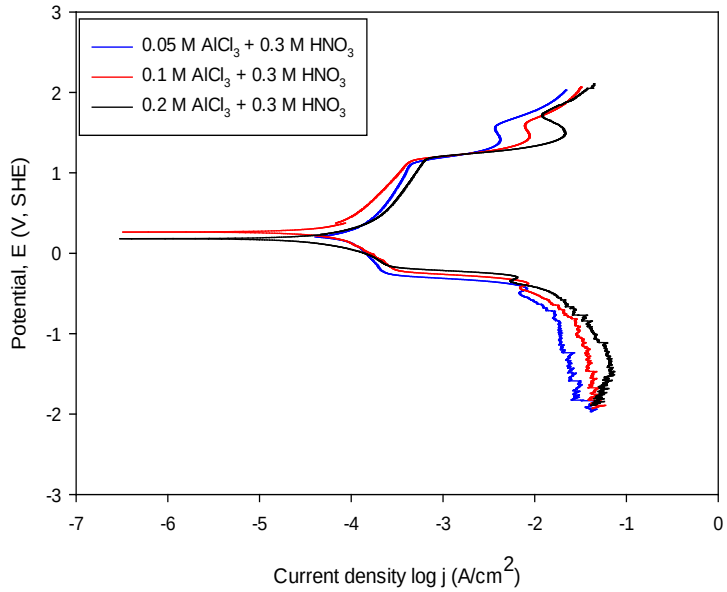

Figure 4.12: Polarisation curve of Pt in 0.05, 0.1 and 0.2 M $AlCl_3$ and 0.3 M HNO_3 at 45 ˚C after nitrogen deaeration

In Figures 4.11 to 4.13 the polarisation curves follow similar trends but there is a gradual increase in the current density for chlorine development, while the potential at which chlorine is developed (about 1.4 V) does not change.

Additional results are shown in Appendix F.

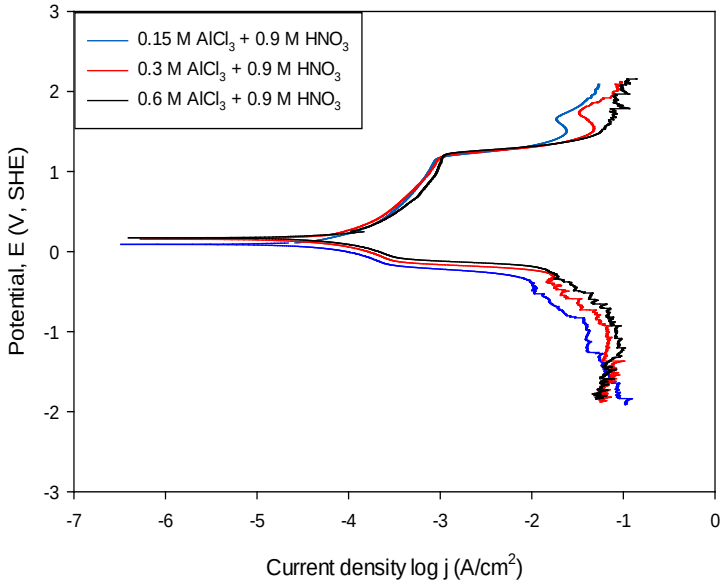

Figure 4.13: Polarisation curve of Pt in 0.15, 0.3 and 0.6 M $AlCl_3$ and 0.9 M HNO_3 at 45 °C after nitrogen deaeration

4.4.4 Electrochemical dissolution of platinum

According to Faraday's law the mass of metal reacted in an electrochemical cell can be obtained from the current flowing:

$$m = \frac{ita}{nF} \qquad (4.19)$$

Where

m = mass of metal reacted in grams

i = current in Ampere (i.e. Coulombs/second)

t = time in seconds

a = atomic mass of Pt (i.e. 195.08 g/mol)

n = number of equivalents exchanged

F = Faraday's constant (96 480 coulombs/equivalent)

In order to relate the electrochemical dissolution with conventional leaching in $AlCl_3/HNO_3$ solutions a calculation of the anodic dissolution of platinum employing Equation 4.19 was applied using Figures 4.12 and 4.13. Electrochemical dissolution of platinum in 0.6 M $AlCl_3$ and 0.9 M HNO_3 at 45 $^{\circ}$C will occur at a current density of 100 mA/cm^2 at a potential just below the onset of chlorine evolution. With the lower concentrations depicted in Figure 4.13 (0.2 M $AlCl_3$ and 0.3 M HNO_3) the maximum current density will be about 32 mA/cm^2.

The following reaction is assumed to take place during the anodic dissolution

$$[PtCl_4]^{2-}_{(aq)} + 2Cl^-_{(aq)} \rightleftharpoons [PtCl_6]^{2-}_{(aq)} + 2e^- \qquad E^0 = -0.74\ V \qquad (4.20)$$

For the case represented by Figure. 4.12 (0.6 M $AlCl_3$ and 0.9 M HNO_3 at 45 °C):

$$m = \frac{0.1 \times 3600 \times 195.08}{4 \times 96480} = 0.18\ g$$

Using the data in Figure 4.13 (0.2 M $AlCl_3$ and 0.3 M HNO_3 at 45 $^{\circ}C$) it is found that 0.06 g of Pt will dissolve.

The careful selection of electrolyte and the potential as well as maintaining a high anodic current is therefore crucial in any practical application of electrochemical leaching techniques.

4.5 Determination of Tafel parameters

Three Tafel parameters are important in the characterisation of electrochemical systems, namely the anodic and cathodic slopes b_a and b_c and the exchange current density (j_0).

4.5.1 Determination of j_0 from Tafel slopes

Figure 4.14 is a schematic Tafel plot indicating that slopes b_a and b_c are obtained by constructing the tangent to the Tafel curves at suitable anodic and cathodic overpotentials. The choice of the points at which the tangents are calculated is problematic as they have to be within the region of pure charge transfer control, and prior close inspection of the polarisation curves is essential before the tangents are drawn. Nevertheless, a large measure or arbitrariness in the choice requires that results are treated with care. For this reason this method was not followed in the present research. An analytic approach was followed in which use was made of the Tafel equation as discussed in Section 4.5.2 below. Using this method the average of the slopes between 10 and 20 mV were used to determine the exchange current density.

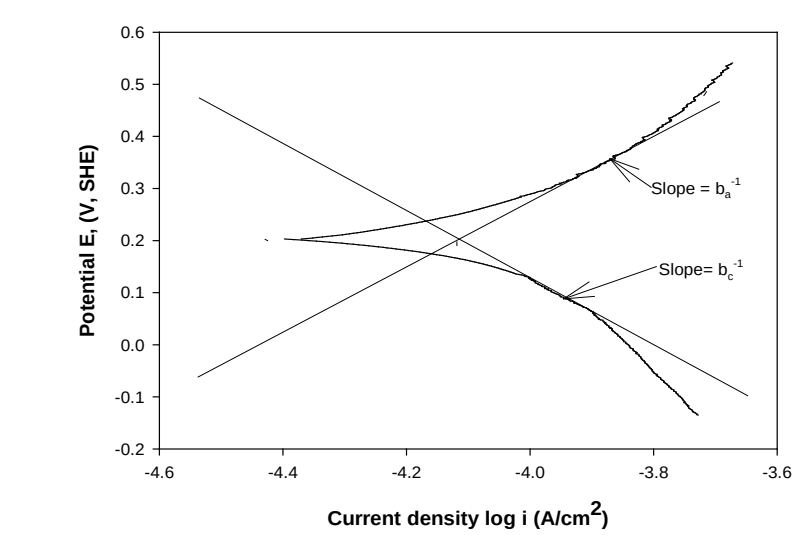

Figure 4.14: Schematic polarisation curves and the determination of Tafel slopes

4.5.2 Determination of j_0 from the Tafel equation

The Tafel equation may be written in the following form for the anodic reaction when the cathodic reaction is negligibly small:

$$j = j_0 \exp \frac{\beta F \eta}{RT} \tag{4.21}$$

From the equation it follows that:

$$\log j = log j_0 - \frac{\beta F \eta}{2.3RT} \tag{4.22}$$

For β = 0.5, R = 8.314 J/m.K and F = 96 500 C/mol it is obtained that:

$$\log j_0 = \log j + 2520 \frac{\eta}{T} \tag{4.23}$$

By calculating the average values of j_0 in the potential range 10 to 20 mV using an Excel spreadsheet, exchange current densities were obtained at the temperatures and electrolyte compositions

4.5.3 Determination of activation energies

As the exchange current density is a measure of the rate of electrochemical reactions on a metal surface at equilibrium, it provides a convenient way to calculate the temperature dependence of the reactions, leading to the calculation of the activation energy. Table 4.3 below shows the calculated exchange current densities of Pt in all the electrolytes.

Table 4.3: Values of j_0 calculated from the Tafel equation

Electrolyte	j_0 (25 °C) A cm^{-2}	j_0 (35 °C) A cm^{-2}	j_0 (45 °C) A cm^{-2}
A	3.15 x 10^{-06}	6.17 x 10^{-06}	3.18 x 10^{-05}
B	2.88 x 10^{-06}	1.62 x 10^{-05}	7.43 x 10^{-05}
C	3.28 x 10^{-06}	3.39 x 10^{-05}	5.20 x 10^{-05}
D	7.94 x 10^{-06}	3.47 x 10^{-05}	1.15 x 10^{-04}
E	1.14 x 10^{-05}	3.05 x 10^{-05}	6.31 x 10^{-05}
F	9.58 x 10^{-06}	3.76 x 10^{-05}	5.13 x 10^{-05}
G	4.65 x 10^{-06}	2.83 x 10^{-05}	1.20 x 10^{-04}
H	2.50 x 10^{-06}	1.89 x 10^{-05}	1.20 x 10^{-04}
I	4.24 x 10^{-06}	2.19 x 10^{-05}	4.01 x 10^{-05}

Legend: $AlCl_3$ + HNO_3: **A**: 0.015M+0.1M; **B**: 0.03M+0.1M; **C**: 0.06M+0.1M; **D**: 0.05M+0.3M; **E**: 0.1M+0.3M; **F**: 0.2M+0.3M; **G**: 0.15M+0.9M; **H**: 0.3M+0.9M; **I**: 0.6M+0.9M

No clear trend can be seen in the values obtained, but in general the exchange current densities increased with increasing temperature and with increasing $AlCl_3$ and HNO_3 concentration.

Activation energies can conveniently be determined by means of the Arrhenius plot, which is a graphic representation of the rate constant of reactions plotted against the reciprocal of the temperature. Figures 4.15 and 4.16 show selected Arrhenius plots for Pt, obtained by the following equations:

$$Rate = A\exp\frac{-E_a}{RT} \qquad (2.52a)$$

Which can also written in the form:

$$\ln j_o = \ln A - \frac{E_a}{R}\frac{1}{T} \qquad (2.52b)$$

Where the rate of the surface reactions are represented by the exchange current densities.

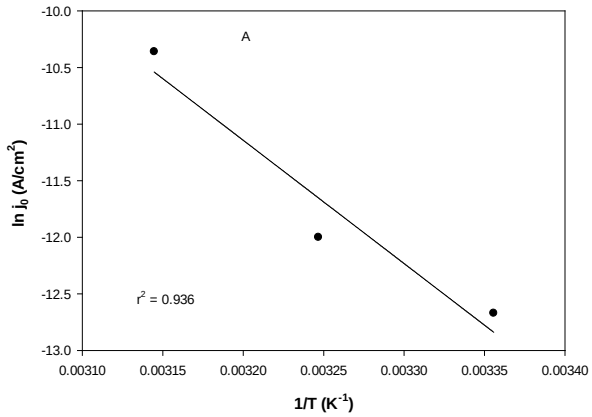

Figure 4.15: Arrhenius plot of Pt in 0.015 M $AlCl_3$ and 0.1 M HNO_3

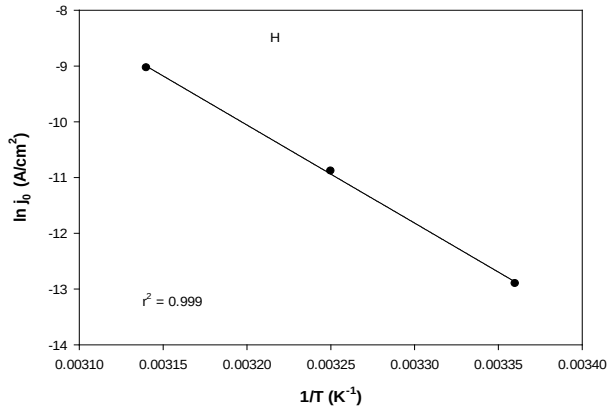

Figure 4.16: Arrhenius plot of Pt in 0.3 M $AlCl_3$ and 0.9 M HNO_3

Table 4.4 below provides information of the activation energies of all the electrolytes. The values of the activation energy range from 85 to 148 kJ/mol, which indicate that Pt dissolution is controlled by surface chemical reactions. No clear trend is, however, discernible.

Table 4.4: Influence of $AlCl_3$ + HNO_3 concentrations on activation energy			
Electrolyte	**Temperature (°C)**	**ln j_0 (A cm^{-2})**	**Activation energy (E_a) kJ/mol**
A	25	-12.67	91
	35	-12.00	
	45	-10.36	
B	25	-12.76	128
	35	-11.03	
	45	-9.51	
C	25	-12.63	105
	35	-10.29	
	45	-9.86	
D	25	-11.74	101
	35	-10.27	
	45	-9.07	
E	25	-11.38	65
	35	-10.40	
	45	-9.67	
F	25	-11.56	63
	35	-10.19	
	45	-9.88	
G	25	-12.28	123
	35	-10.47	
	45	-9.03	
H	25	-12.90	146
	35	-10.88	
	45	-9.13	
I	25	-12.37	85
	35	-10.73	
	45	-10.12	

Legend: $AlCl_3$ + HNO_3: **A**: 0.015M+0.1M; **B**: 0.03M+0.1M; **C**: 0.06M+0.1M; **D**: 0.05M+0.3M; **E**: 0.1M+0.3M; **F**: 0.2M+0.3M; **G**: 0.15M+0.9M; **H**: 0.3M+0.9M; **I**: 0.6M+0.9M

4.5.4 Summary

With regard to the electrochemical investigation use was made of linear polarisation. In the anodic curves there was evidence of a competition between nitrate ions and chloride ions for sites on the Pt surface, firstly leading to the formation of platinum oxides with eventual chlorine and oxygen evolution. The cathodic polarisation curves indicated hydrogen evolution, reduction of surface oxide films and nitrate ion reduction on the electrode surface. From the composite polarisation curves the Tafel plots were constructed and exchange current densities were

obtained. The exchange current densities were used to calculate the activation energies by means of Arrhenius plots, which indicated that at high electrolyte concentrations higher exchange current densities resulted.

4.6 Leaching study

The electrolyte concentrations used for the recovery of platinum are shown in Table 3.3. The temperatures investigated were 25, 35 and 45 °C for a 24 h leaching period. It was found that only the solutions with the higher concentrations of $AlCl_3$ and HNO_3 (0.6 M $AlCl_3$ and 0.9 M HNO_3) gave meaningful results, which are shown in Figures 4.17 to 4.19. The rest of the solutions, even at 45 °C, did not recover more than 10% Pt. This result is in accordance with the findings of Letowski and Distin (1985, 1987) who obtained low recoveries with HNO_3 concentrations below 0.7 M. The regression lines shown in Figures 4.17 to 4.19 were obtained by fitting the experimental results to the following polynomial equation:

$$\text{Percentage recovery} = \frac{t}{a + bt} \qquad (4.24)$$

Where t is time (h) and a and b are constants.

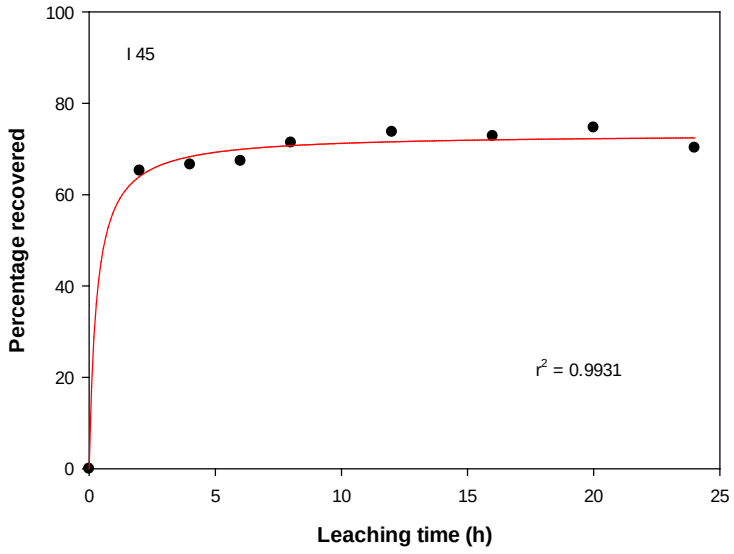

Figure 4.17: Platinum recovery in 0.6 M $AlCl_3$ and 0.9 M HNO_3 lixiviant at 45 °C

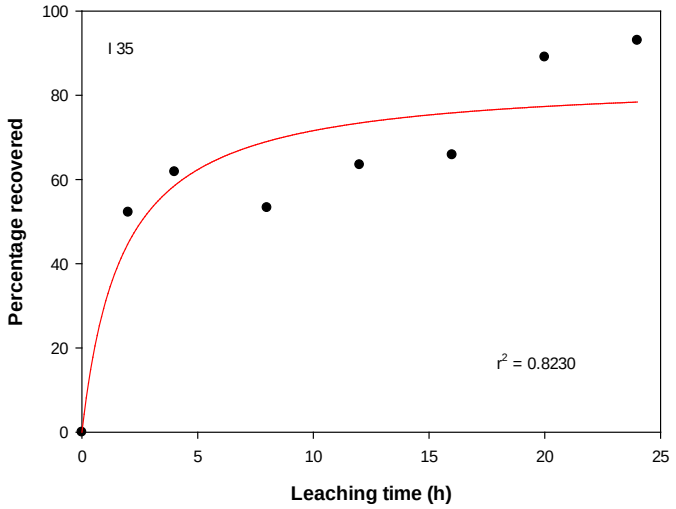

Figure 4.18: Platinum recovery in 0.6 M $AlCl_3$ and 0.9 M HNO_3 lixiviant at 35 °C.

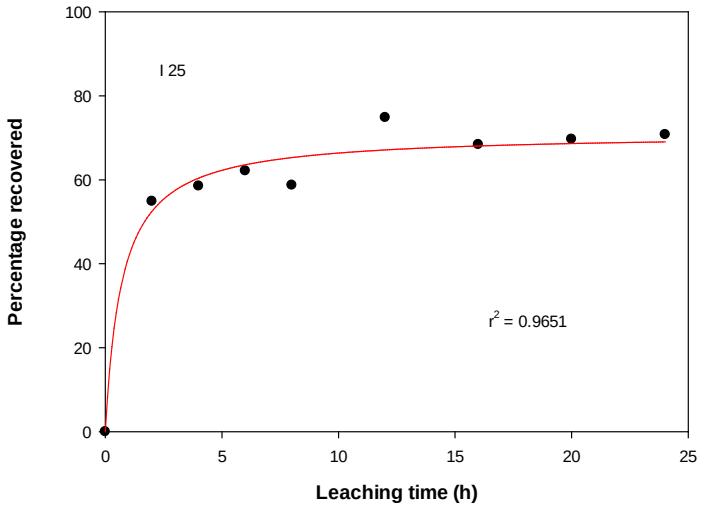

Figure 4.19: Platinum recovery in 0.6 M $AlCl_3$ and 0.9 M HNO_3 lixiviant at 25 °C

The relatively low recoveries shown in Figures 4.17 to 4.19 might be attributed to several effects relating to, *inter alia* the experimental conditions. One aspect that was briefly investigated was the presence of Pt on the finely-divided substrate material residue after rinsing. A dried specimen was subjected to an energy-dispersive X-ray spectroscopic analysis in an electron microscope. Pt was detected to a level of 10 atomic % on the surface of the specimen. This may be the result of inefficient rinsing, as well as the possibility of platinum chloro-complexes having been hydroxylated due to the washing with pure water, instead of using electrolyte. Shams *et al.*

(2004) reported adsorption platinum complexes onto reactor walls after prolonged contact with lixiviants.

4.6.1 Summary

The leaching study showed that electrolytes A and F (refer to Table 3.3) could not achieve reasonable amounts of Pt from the test material, even if the temperature was raised to 45 °C. A similar result was found in the literature where it is reported that chloride/HNO_3 electrolytes could not achieve acceptable recoveries at acid concentrations below 0.7 M. The results show that at high chloride and nitric acid concentrations (0.6 M $AlCl_3$ and 0.9 M HNO_3) and a temperature of 45 °C platinum recoveries were still well below 80%. The reason for these relatively low levels of platinum recovery can possibly be ascribed to adsorption of hexachloroplatinate complex $[PtCl_6]^{2-}$ on the filtration residue and/or desolubilisation of $[PtCl_6]^{2-}$ due to hydroxylation during rinsing.

CHAPTER 5: CONCLUSIONS AND RECOMMENDATIONS

5.1 CONCLUSIONS

Environmental concerns led to the introduction of platinum in automotive catalytic converters in order to diminish the negative environmental impact of exhaust gases. With the increased use of PGM-containing autocatalysts, the reclaiming of PGMs from spent catalysts is becoming essential. To this end hydrometallurgical processing to recover platinum is gaining importance because it is environmentally more acceptable compared to, for example, pyrometallurgical techniques and those based on the use of dangerous chemicals, such as cyanides and aqua regia. The use of halide ions as complexing agents provide potential alternatives, especially also with regard of the economics of these processes. Particularly attractive methods are those based the use of halide ions from simple salts, e.g. sodium chloride or aluminium chloride, in conjunction with nitric acid.

The construction of Pourbaix diagrams of Pt in chloride environments confirmed that stable chloro-complexes $[PtCl_4]^{2-}$ and $PtCl_6]^{2-}$, as well as platinum oxides (PtO and PtO_2) could play a role under the experimental conditions employed in this study. From the thermodynamic results it can be concluded that the systems deserving consideration favour high chloride concentration and low temperatures.

The picture of Pt speciation which has resulted from the work of a large number of researchers is one in which the initial reaction (aquo ligand exchange of chloride ions) is rapid and also reversible, while subsequent reactions, namely hydroxide ion ligand exchange of chloride and aquo ligands are relatively slow. High chloride-containing complexes are more stable in acid solutions and high chloride concentrations, resulting in $[PtCl_6]^{2-}$ as the main species under these conditions.

From the electrochemical polarisation curves, the influence of the concentrations of HNO_3 and $AlCl_3$, as well as temperature and deaeration on the platinum electrode kinetics could be determined.

The most prominent features of the anodic polarisation curves could be described in terms of published electrode potentials. Notable reactions were the adsorption of chloride on the Pt surface and the gradual formation of $[PtCl_6]^{2-}$, followed by the formation of Pt oxides at 1.00 to 1.01 V There is evidence (also supported by literature) of a competition between nitrate ions and chloride ions for sites on the Pt surface, with increasing anode potential first leading to the formation platinum chloro-complexes, then to of platinum oxides and eventually to chlorine and oxygen evolution.

Possible cathodic reduction reactions to be considered are: hydrogen evolution, reduction of dissolved oxygen to hydrogen dioxide, nitrate ion reduction to nitrite, nitrite ion reduction to nitric oxide, and Pt oxide reduction. Near the equilibrium potential the dominant reactions are probably the progressive physical and chemical adsorption of mainly hydrogen ions onto the platinum surface, followed by hydrogen evolution. Evidence was found for the reduction of dissolved oxygen to hydrogen dioxide at about 1.3 V. The presence of oxygen in the electrochemical cells was possibly due to ingress of air into the electrolytic cell during polarisation or inadequate deaeration before polarisation. The initial cathodic nitrate reduction step is the reduction of nitrate to nitrite at -0.01 V. At a potential of -0.46 V nitrate is probably reduced to NO while at -0.85 V reduction to N_2O_4 seems possible. Reduction of surface Pt oxide films PtO and PtO_2 occurred at -1.00 V and 1.01 V, respectively.

The values of the exchange current densities were obtained by application of the Tafel equation. No clear trend could be seen in the values obtained, but in general the exchange current densities increased with increasing temperature and with increasing $AlCl_3$ and HNO_3 concentration. The exchange current density values obtained were in the range 2.5 to 9.6 $\mu A/cm^2$ at 25 °C, from 6.2 to 16.2 $\mu A/cm^2$ at 35 °C and from 74 to 115 $\mu A/cm^2$ at 45 °C. The activation energies obtained for 7 of the 9 electrolytes were in range expected for chemical reactions, namely 85 to 146 kJ/mol.

Leaching of platinum by lixiviants containing 0.6 M $AlCl_3$ and 0.9 M HNO_3 resulted in recoveries, after 24 h, of about 70%, even at 45 °C. The reason for these relatively low levels of platinum recovery can possibly be ascribed to adsorption of the hexachloroplatinate complex $[PtCl_6]^{2-}$ on the filtration residue and/or desolubilisation of $[PtCl_6]^{2-}$ due to hydroxylation during water rinsing when the pH increased. The dissolution of Pt as its chloro-complexes is limited by the occurrence of Pt oxyhydrate at neutral to basic pH (Harjanto *et al.* 2006). From leaching results it can be concluded that with high concentration of chloride ion and nitrate ion and at the higher temperature the recovery of platinum was increased, but that the total recovery of platinum remained unsatisfactory.

5.2 ATTAINMENT OF OBJECTIVES

In order to achieve the aims of this study, the following objectives had to be met:

5.2.1 The major research question

Identification of the electrochemical reactions of Pt in different mixtures of aluminium chloride and nitric acid at different temperatures using potentiostatic techniques.

The major research question has been answered within the limitations imposed by the equipment available to the study.

Notable anodic reactions found were the adsorption of chloride on the platinum surface and the gradual formation of $[PtCl_6]^{2-}$, followed by the formation of platinum oxides at 1.00 to 1.01 V. The results show that anodic currents diminished with lower chloride concentrations. A seemingly anomalous anodic behaviour at 35 °C and 45 °C could be explained in terms of a competition between platinum oxide formation and the formation of platinum chloro-complexes. Evidence for the following cathodic reduction reactions were found: hydrogen evolution, reduction of dissolved oxygen to hydrogen dioxide (-1.3 V SHE), nitrate ion reduction to nitrite (-0.01 V SHE), nitrite ion reduction to nitric oxide (-0.85 V SHE) and reduction of PtO and PtO_2 to Pt (at -1.00 V and 1.01 V SHE, respectively).

5.2.2 Sub-problem 1

Determination of stability regions of Pt complexes by constructing the relevant Pourbaix diagrams.

Sub-problem 1 has been adequately solved by the successful construction of Pourbaix diagrams for the system Pt-Cl-H_2O at temperatures ranging from 25 to 45 °C.

From the thermodynamic results it could be concluded that the systems deserving consideration favour high chloride concentration and high temperatures.

5.2.3 Sub-problem 2

Recovery of Pt from a virgin autocatalytic system using $AlCl_3/HNO_3$-containing lixiviants at temperatures ranging from 25 to 45 °C.

As a brief exploratory investigation Sub-problem 2 was partially successful in that the limitations of the $AlCl_3/HNO_3$ could be established.

The brief study showed that the recovery of Pt was low for mixtures with low chloride concentrations, which could be expected from the electrochemical polarisation curves obtained in electrolytes with different chloride concentrations. The maximum platinum recovery attained, was 60% at 45 °C in a mixture containing 0.6 M $AlCl_3$ and 0.9 M HNO_3.

5.3 RECOMMENDATIONS

In further investigations regarding the dissolution of platinum from spent catalytic converters, it is suggested that the following work can be contemplated:

- For electrochemical study, the effect of temperature and concentration should be investigated, where the chloride concentration can be kept constant with variation in the nitric acid concentration in order to further elucidate the synergistic effects.
- The lixiviant composition should be optimised in order to attain Pt recoveries of near 100%.
- The sampling and sample preparation procedures in leaching studies should be examined in order to achieve less scatter in the results.
- There should be an effort to correlate the results of the electrochemical investigation with the findings of the leaching experiment

REFERENCES

Angelidis, T.N. and Skouraki, E. 1996. Preliminary studies of platinum dissolution from a spent industrial catalyst, Applied catalysis A: general, 142 (2): 387-395.

Aprahamian, V. H. and Demopoulos, G. P. 1995. The solution chemistry and solvent extraction behavior of Cu, Fe, Ni, Zn, Pb, Sn, Ag, As, Sb, Bi, Se, and Te in acid chloride solutions reviewed from the standpoint of PGM refining, Mineral processing and extraction metallurgy review. 14, 143-167.

ASM International. 1987. Metals Handbook, Volume 13 (Corrosion). Metals Park, Ohio.

Atkins, P. and de Paula, J. 2006 Atkins' Physical chemistry 8th edition, Oxford University Press New York.

Atkinson, G. B., Desmond, D. P., Kuczynski, R. J. and Walters, L. A. 1989. Recovery of PGM from Virgin Automotive Catalysts by Cyanide Leaching, Oral Presentation, Proc. Int. Precious Met. Inst., Las Vegas NV.

Azaroul, M., Romand, B., Freyssinet, P. and Disnar, J-R. 2001. Solubility of platinum in aqueous solution at 25 °C and pHs 4 to 10 under oxidizing conditions, Geochimica Acta, 65 (24): 4453-4466.

Baghalha, M. 2007. Leaching of an oxide gold ore with chloride/ hypochlorite solutions, International Journal of Processing, 82: 178-186.

Baghalha, M., Gh, H. K. and Mortaheb, H. R. 2009. Kinetics of platinum extraction from spent reforming catalysts in aqua regia solutions, Hydrometallurgy, 95: 247-253.

Barakat, M. A., Mahmoud, M. H. H. 2004. Recovery of platinum from spent catalyst, Hydrometallurgy, 72: 179-184.

Bard, A. J. and Faulkner, L. R. 1980. Electrochemical methods fundamentals and applications, John Wiley and Sons. United State of America.

Bautista, R.G., Yue, L., Tyson, D.R. 1989. Platinum and Palladium Recovery from Spent Automotive Catalysta, Leachinq with (HCl):(HNO_3) in a Packed and Fluidized Bed. In: Torma, A. E., Gundiler, I. H. (Editors), precious, Rare Metal Technologies, Process Metallurgy, 2: 345-363.

Benke, G. and Gnot, W. 2002. The electrochemical dissolution of platinum, Hydrometallurgy, 64: 205–218.

Bernadis, F. L., Grant, R. A. and Sherrington, D. C. 2005. A review of methods of separation of the platinum- group metals through their chloro-complexes, Reactive and Functional polymers, 65: 205-217.

Bolonski, L. and Distin, P. A. 1991. Platinum and Rhodium Recovery from Scrapped Honeycomb autocatalyst by Chloride leaching and hydrogen reduction, Precious, 179-189.

Bolonski, L. and Distin, P. A. 1992. Platinum group metals Recovery from recycled Autocatalyst by Aqueous Processing, Extractive Metallurgy of gold and Base Metals, 277-280.

Breuer, P. L. and Jeffrey, M. I. 2002. An electrochemical study of gold leaching in thiosulphate solutions containing copper and ammonia, Hydrometallurgy, 65: 145- 157.

Chen, J. and Huang, K. 2006 “A New Technique for Extraction of Platinum Group Metals by Pressure Cyanidation”, Hydrometallurgy, 82, 164–171. (cited by Jha, M. K., Lee, J., Kim, M., Jeong J., Kim, B-S., Kumar, V. 2013. Hydrometallurgical recovery/recycling of platinum by the leaching of spent catalysts: A review, Hydrometallurgy, 133: 23–32).

Cotton, F.A. and Wilkinson, G. 1988. Advanced Inorganic Chemistry, A Comprehensive text, 5th Edition, Wiley.

CRC Handbook of Chemistry and Physics 2011-2012, (92nd Edition), CRC Press.

De Aberasturi, D. J., Pinedo, R., de Larramendi, I. R., de Larramendi, J. I. R. and Rojo, J. 2011. Recovery by hydrometallurgical extraction of the platinum-group metals from car catalytic converters, Minerals engineering, 24: 505-513.

De Sá Pinheiro, A. A., de Lima, T. S., Campos, P. C. and Afonso, J. C. 2004. Recovery of platinum from spent catalyst in a fluoride- containing medium, Hydrometallurgy, 74: 77-84.

Desmond, D. P., Atkinson, G. B., Kuczynski, R. J., and Walters, L. A. 1991. High-temperature Cyanide Leaching of Platinum Group Metals from Automobile Catalysts – Laboratory Tests, Report of Investigations, US Bureau of Mines, 9384.

Distin, P.A. and Letowski, F. K. 1984. Recovery of precious metals from materials containing same, (Patent: CA 1228989).

Dragulovic, S., Dimitrijevic, M., Kostov, A. and Jakovljevic, S. 2008. "Recovery of platinum group metals from spent automotive catalyst" 12th International Research/ Expert Conference, "Trends in the Development of Machinery and Associated Tecbnology", Istanbul, Turkey, 26-30 August.

Elding, L. 1970. Acta Chem. Scand., 24, 1331-1527.

Fenger, J. 1999. Urban air quality, Atmospheric environment, 33: 4877-4900.

Fornalczyk, A. and Saternus, M. 2009. Removal of platinum group metals from the used auto catalytic converter, Metalurgija, 48 (2): 133-136.

Goldschmidt, V. M. 1954. Geochemistry, Oxford University Press, Oxford.

Greenwood, N. N. and Earnshaw, A. 1984. Chemistry of the elements. Oxford: Pergamon Press Limited.

Gupta, C. K. and Mukherjee, T. K. 1990. Hydrometallurgy extraction processes, vol 1, India: CRC Press.

Gwicana, S. 2007. Micellar-enhanced ultrafiltration of palladium and platinum anions, Port Elizabeth: NMMU. (Dissertation-Msc).

Han, K. N. 2007. Recovery of precious metals, (US Patent 7166145B1).

Han, K. N. and Meng, X. 1996. Recovery of platinum group metals and rhenium from materials using halogen reagents, (Patent: US 5542957).

Harabayashi, S., Kroll, C. N. and Nowak, D. J. 2012. Developmental of a distributed air pollutant dry deposition modeling framework, Environmental pollution, 171: 9-17.

Harjanto, S., Cao, Y., Shibayama, A., Naitoh, I., Nanami, T., Kasahara, K. M., Okumura, Y., Liu, K. and Fujita, T. 2006. Leaching of Pt, Pd and Rh from automotive catalyst residue in various chloride based solutions, Materials Transactions, 47 (1): 129-135.

Hartley, F. R. 1991. Chemistry of the platinum group metals recent developments, Elsevier New York.

Heck, R. M. and Farrauto, R. J. 2001. Automobile exhaust catalysts, Applied catalysis A: General, 221: 443-457.

Hilson, G. and Monhemius, A. J. 2006. Alternatives to Cyanide in the Gold Mining Industry: What Prospects for the Future? Journal of cleaner production, 14: 1158-1167.

Hoffman, J. E., 1988a. Recovering platinum-group metals from auto catalysts, Journal of metals, 40: 40-44.

Hoffmann, J. E., 1988b. Recovery of platinum group metals from automotive catalysts, Precious and rare metal technologies, 345-363.

HSC Chemistry 6.1 2006. Ontokumpu Research Oy, Antti Roine manual handbook.

Huang, K., Chen, J., Chen Y.-R., Zhao, J.-C., Li, Q.-W. and Yang, Q.-X. 2006. Recovery of precious metals from spent autocatalysts by method of pressure alkaline treatment- cyanide leaching, China. Journal. Nonferrous Metallurgy 16 (2): 363–369.

Jafarifar, D., Daryanavard, M. R. and Sheibani, S. 2005. Ultra fast microwave-assisted leaching for recovery of platinum from spent catalyst, Hydrometallurgy, 78: 166-171.

Jha, M. K., Lee, J., Kim, M., Jeong J., Kim, B-S. and Kumar, V. 2013. Hydrometallurgical recovery/recycling of platinum by the leaching of spent catalysts, A review. Hydrometallurgy, 133: 23–32.

Kalavrouziotis, I. K. and Koukoulakis, P. H. 2009. The environmental impact of the platinum group elements (Pt, Pd, Rh) emitted by the automobile catalyst converters. Water air soil pollution, 196: 393-402.

Kear, G. and Walsh, F. C. 2005. The characteristics of a true Tafel slope, Corrosion and Materials, 30 (6): 51-55.

Kelly, R. G., Scully, J. R., Shoesmith, D. W. and Buchheit, R. G. 2002. Electrochemical techniques in corrosion, Science and Engineering, New York: Marcel Dekker.

Khaled, K. F. 2010. Studies of iron corrosion inhibition using chemical,electrochemical and computer simulation techniques, Electrochimica Acta, 55: 6523-6532.

Kizilaslan, E, Aktaş, S. and Şeşen, M. K. 2009. Towards environmentally safe recovery of platinum from scrap automotive catalytic converters, Turkish J. Eng. Env. Sci., 33: 83-90.

Kobel, P. 2010. "Catalytic combustion of CO and HC". Laboratory of combustion and fuels, http://fluid.wme.pwr.wroc.pl/~spalanie/dydaktyka/combustion_lab/combustion_lab_manual_catal Accessed: 15 November 2013.

Lambert, J.-F., Marceau, E. Shelimov, B. Lehman, J.,Le Be de Penguily, V., Carrier X., Boujday, S., Pernot, H. and Che, M. 2000.Thermal chemistry of oxide-supported platinum catalysts: A comparative study, Studies in surface. Science.and catalysis, 130: 1043-1048.

Lassi, U. 2003. Deactivation correlations of Pd/Rh three-way catalysts designed for Euro IV emission limits, Oulu University Press (Thesis - Ph.D.).

Letowski, F. K. and Distin, P. A. 1985. Platinum and palladium recovery from spent catalysts by aluminium chloride leaching, Recycle and secondary recovery of metals, 735-745.

Letowski, F. K. and Distin, P. A. 1987. Platinum and palladium recovery from scrapped catalytic converters by a chloride leach route - laboratory results and pilot plant design. Separation processes in Hydrometallurgy, 68-76.

Letowski, F. K. and Robinson, R. E. G. 1990. “A process for extracting precious metals from an ore concentrate” (Patent: ZA 90/9059).

Li, F. B., Hillman, A. R, Lubetkin, S. D. and Roberts, D. 1992. Electrochemical quartz crystal microbalance studies of potentiodynamic electrolysis of aqueous chloride solution: surface processes and evolution of, Journal of. Electroanalytical Chemistry, 335: 345-362.

Littauer, E. L. and Shreir L.L. 1966. Anodic polarisation of platinum in sodium chloride solutions, Electrochimica Acta, 11: 527-536.

Loferski, P. 2008. Platinum-group metals Minerals yearbook. USGS Science for a changing world.

Loferski, P. 2011. Platinum-group metals Minerals yearbook. USGS Science for a changing world.

Mahmoud, M. H. H. 2003. Leaching platinum- group metals in a sulfuric acid/ chloride solution, Journal of metals, 55: 37-40.

Mang, T., Breitscheidel, B., Polanek, P. and Knözinger, H. 1993. Applied catalysis A: General, 106: 239-258. (cited by Spieker, W. A., Liu, J., Miller, J. T., Kropf, A. J. and Regalbuto, J. R. 2002. An EXAFS study of the co-ordination chemistry of hydrogen hexachloroplatinate (IV) 1. Speciation in aqueous solution, Applied catalysis A: General 232: 219-235)

Marinho, S. R., Afonso, J. C., and da Cunha, J. W. S. D. 2010. Recovery of platinum from spent catalysts by liquid-liquid extraction in chloride medium, Journal of hazardous materials, 179: 488-494.

McCafferty, E. 2005. Validation of corrosion rates measured by the Tafel extrapolation method, Corrosion Science, 47: 3202-3215.

Miolati, A. and Pendini, U. 1903. Z. Anorg. Chem. 33: 251 (cited by Spieker, W. A., Liu, J., Miller, J. T., Kropf, A. J. and Regalbuto, J. R. 2002. An EXAFS study of the co-ordination chemistry of hydrogen hexachloroplatinate (IV) 1. Speciation in aqueous solution, Applied catalysis A: General 232: 219-235).

Mishra, R. K. 1988. Recovery of platinum group metals from automobile catalytic converters- A Review, Precious metals ’89, The minerals, metals and materials society, 483-501.

Mogwase, B. M. S. 2012. An electrochemical study of the oxidation of platinum employing ozone as oxidant and chloride as complexing agent, North-West University (Dissertation- MSc).

Oh, C. J., Lee, S. O., Yang, H. S., Ha, T. J., and Kim, M.J. 2003. Selective leaching of valuable metals from waste printed circuit boards, Journal of air and waste management association 53: 897-902.

Osseo-Asare, K., te Riele, W., Ndlovu, S. and van Dyk, L. 2010. Leaching process in hydrometallurgy, Course 30- 3 September manual.

Patil, R. S., Juvekar, V. A. and Naik, V. M. 2011. Oxidation of chloride ion on platinum electrode: dynamics of electrode passivation and its effect on oxidation kinetics, Ind. Eng. Chem. Res, 50: 12946-12959.

Platinum 2008, Johnson Matthey, ISSN 0268-7305.

Platinum 2013, Johnson Matthey, ISSN 0268-7305.

Pletcher, D. 2009. A First Course in Electrode Processes. RSC Publishing, Cambridge.

Priyantha, N. and Malavipathirana, S. 1996. Effect of chloride ions on the electrochemical behaviour of platinum surfaces, J. Natn. Sci. Council Sri Lanka, 24 (3): 237-249.

Puvvada, G. V. K. and Murthy, D. S. R. 2000. Selective precious metals leaching from a chalcopyrite concentration using chloride/ hypochlorite media, Hydrometallurgy, 58: 185-191.

Rao, C. R. M. and Reddi, G. S. 2000. Platinum group metals (PGM); occurrence, use and recent trends in their determination, Trends in analytical chemistry, 19: 565-586.

Ravera,, S. B. and Chavez, M. A. 2005. Optimization of Physico-Chemical Models using the Gauss-Newton Method, Journal Chil. Chemical Society, 50 (4):739-743.

Ravindra, K., Bencs, L. and van Grieken, R. 2004. Review: Platinum group elements in the environment and their health risks, University of Antwerp. Belgium:1-9.

Rieger, P. H. 1987. Electrochemistry, Englewood Cliffs, NJ. Prentice-Hall.

Roine, A. and Anittila, K. 2006. HSC Chemistry 6.1.Outokumpu research, Qutotec

Shams, K., Beiggy, M. R. and Shirazi, A. G. 2004. Platinum recovery from a spent industrial dehydrogenation catalyst using cyanide leaching followed by ion exchange, Applied catalysis A: General, 254: 227-234.

Shelef, M. and McCabe, R. W. 2000. Twenty-five years after introduction of automotive catalysts: what next?, Catalysis Today, 62: 35-50.

Shelimov, B. N., Lambert, J.-F., Che, M. and Didillon, B. 2000. Molecular-level studies of transition metal–support interactions during the first steps of catalysts preparation: platinum speciation in the hexachloroplatinateralumina system, Journal of Molecular Catalysis A: Chemical 158: 91–99.

Sheng, P. P. and Etsell, T. H. 2007. Recovery of gold from computer circuit board scrap using aqua regia, Waste management and research 25: 380-383.

Silen, L. G. and Martell, A. E. 1971. The stability constants of metal ion complexes, special publication No. 25 (suppl.1), The chemical society, Burlington house, London (cited by Spieker, W. A., Liu, J., Miller, J. T., Kropf, A. J. and Regalbuto, J. R. 2002. An EXAFS study of the co-ordination chemistry of hydrogen hexachloroplatinate (IV) 1. Speciation in aqueous solution, Applied catalysis A: General 232: 219-235)

Song, C. and Zhang, J. 2008. PEM fuel cell electrocatalysts and catalyst layers, Fundamentals and Applications, Springer.

Sousanis, J. 2011. World vehicle population tops 1 billions units. WardsAuto. August 15, http://wardsauto.com/ar/world_vehicle_population_110815.

Spieker, W. A., Liu, J., Miller, J. T., Kropf, A. J. and Regalbuto, J. R. 2002. An EXAFS study of the co-ordination chemistry of hydrogen hexachloroplatinate (IV) 1. Speciation in aqueous solution, Applied catalysis A: General 232: 219-235.

Trasatti, S. 2006. Electrokinetics, University of Milan Italy 23-31.

Trethewey, K. R. and Chamberlain, J. 1995. Corrosion for science and engineering, 2nd edition Harlow, Longman.

Tyson, D. R. and Bautista, R. G. 1987. Leaching kinetics of platinum and palladium from spent automotive catalysts, Separation science and technology, 22 (2 and 3): 1149-1167. (cited by Furimsky, E. 1996.Spent refinery: environment, safety and utilization, Catalysis Today, 30 (4): 223-286).

Upadhyay, A. K., Lee, J-c., Kim, E-y., Kim, M-s., Kim, B-s. and Kumar, V. 2013. Leaching of platinum group metals (PGMs) from spent automotive catalyst using electro-generated chlorine in HCl solution, Journal of chemical technology and biotechnology, 88 (11): 1991-1999.

West, J. M. 1965. Electrodeposition and corrosion processes, London: D. van Nostrand Company limited.

Whitfield, M. 1974. Thermodynamic limitations on the use of the platinum electrode in E_h measurements. Limnology and oceanography, 19: 857-865.

Xie, X., Meng, X. and Han, K. N. 1996. Leaching behavior of palladium in thiourea/ acid solutions. Minerals and metallurgical processing, 13 (3): 119-123.

Zaki, A. 2006. Principles of corrosion engineering and corrosion control, Boston: Elsevier.

Zanjani, A. and Baghalha, M. 2009. Factors affecting platinum extraction from used reforming catalysts in iodine solutions at temperatures up to 95 $^{\circ}$C, Hydrometallurgy, 95: 119-125.

Appendix A Standard free energies of formation of platinum complexes

$$\Delta G^o = -2.303\ RT \log \beta$$

Where R = 8.314 J/K.mol and T = 298.15 K

For example, for $[PtCl_4]^{2-}$ (Table 3.1)

$$\Delta G^o = -2.303\ RT \log \beta$$

$$= -2.303.\ (8.314\ J/K.mol).\ (298.15\ K).\ (13.80)$$

$$= -78.780\ kJ/mol$$

For $[PtCl_6]^{2-}$

$$\Delta G^o = -2.303\ RT \log \beta$$

$$= -2.303.\ (8.314\ J/K.mol).\ (298.15\ K).\ (-24.70)$$

$$= 141\ kJ/mol$$

Therefore, if we consider the formation of $PtCl_4^{2-}$ and $PtCl_6^{2-}$ from its elements, the standard Gibbs free energy can be calculated as follows

$Pt^{2+} + 4Cl^- \rightarrow [PtCl_4]^{2-}$

$\rightarrow \Delta G^o = -78.780\ kJ/mol = G^o[PtCl_4^{2-}] - G^o[Pt^{2+}] - 4.G^o[Cl^-]$

Therefore, $G^o[PtCl_4]^{2-} = \Delta G^o + G^o[Pt^{2+}] - 4.G^o[Cl^-]$

$= \Delta G^o + H^o[Pt^{2+}] - T.S[Pt^{2+}] + 4.H^o[Cl^-] - T.S[Cl^-]$

$= -78.780 + 243.55 - 298.15\ (-9.0E\text{-}02) + 4.(-167.08) - 298.15\ (5.6735E\text{-}02)$

$= -545.52\ kJ/mol$

$Pt^{2+} + 6Cl^- \rightarrow [PtCl_6]^{2-}$

$\rightarrow \Delta G^o = -141\ kJ/mol = G^o[PtCl_6^{2-}] - G^o[Pt^{2+}] - 6.G^o[Cl^-]$

Therefore, $G^o[PtCl_6^{2-}] = \Delta G^o + G^o[Pt^{2+}] - 6.G^o[Cl^-]$

$= \Delta G^o + H^o[Pt^{2+}] - T.S[Pt^{2+}] + 6.H^o[Cl^-] - T.S[Cl^-]$

= -78.780+ 243.55 – 298.15 (-9.0E-02) + 6.(-167.08) – 298.15 (5.6735E-02)

= -755.58 kJ/mol

Appendix B Sample calculation of percentage Pt recovery

Assume a Pt loading of 0.90 wt%, 15 grams of sample leached in a 500 mℓ flask, 10 mℓ of sample made up to 100 ml from which an aliquot is analysed in the ICP, and a Pt concentration of 26.11 mg/ℓ found:

The amount of Pt contained in the 500 mℓ flask will be $\frac{0.90\,x\,15}{100} = 135.00\frac{mg}{500}m\ell = 270.00\frac{mg}{\ell}$.

26.11 mg/ℓ Pt will amount to a total of 5 x 26.11 = 130.55 mg/ℓ in the 500 mℓ flask. This will indicate a recovery of $\frac{130.55\,x\,100}{270.00} = 48.35\%$

Appendix C: Calibration for ICP determination of Pt concentration in leaching samples

Date of Fit: 18/01/2012 15:53:15 Type of Fit: Linear Weighting: 1/Conc

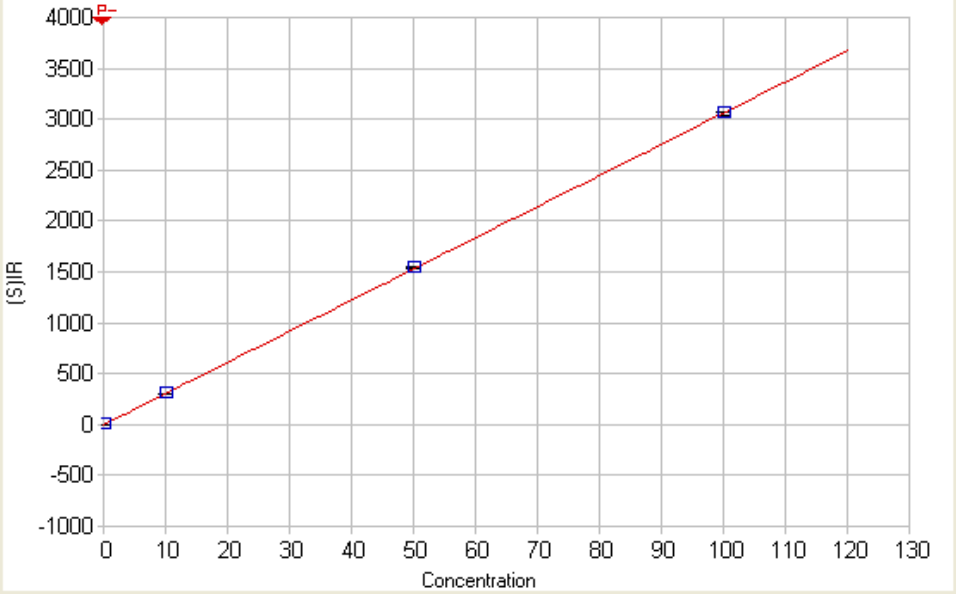

Details:

A0 (Offset):	-0.331542
A1 (Gain):	30.607197
A2 (Curvature):	0.000000
n (Exponent):	1.000000
Correlation:	0.999990
Std Error of Est:	1.246703
MDL:	0.122197
MQL:	0.407323

Status: OK.

Re-Slope:	1.000000
Y-int:	0.000000

☐ Line Switch

Print Limits: ☐ High ☐ MDL ☐ MQL ☑ Low

Cursor:

(S)IR:

Conc:

	Standard Name	Concentration		Difference		Signal		Emphasis
		Stated	Found	Diff	%	(S)IR	Std Dev	
1	Blank	.00000	-.00006	.000	.000	-.33333	.456	1
2	10PPM	10.000	10.030	.030	.297	306.65	2.43	1
3	50PPM	50.000	50.318	.318	.636	1539.8	4.88	1
4	100PPM	100.00	99.652	-.348	-.348	3049.7	19.6	1

Appendix D Pourbaix diagrams of Pt with chloride

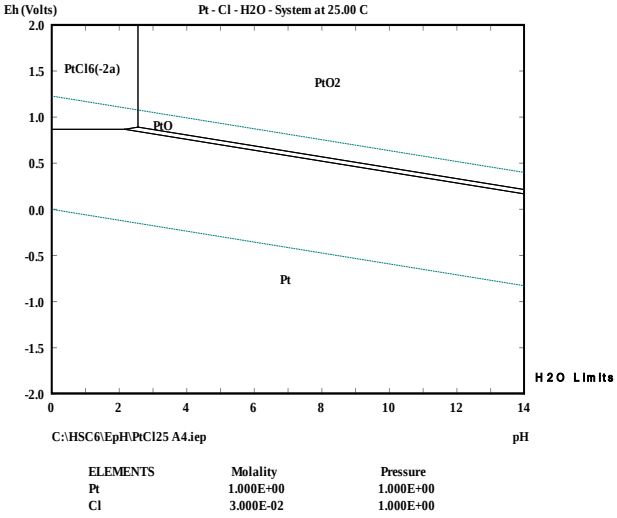

Figure D.1: E_h-pH diagram of Pt- Cl- H_2o system for 0.03 M $AlCl_3$ + 0.1 M HNO_3 concentration at 25^{o}C.

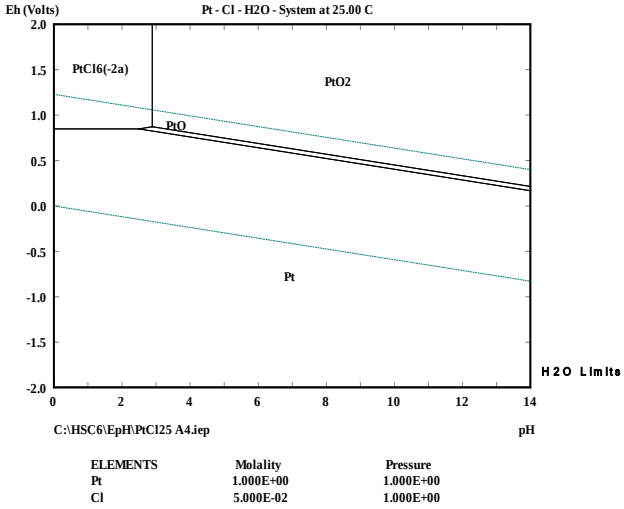

Figure D.2: E_h-pH diagram of Pt- Cl- H_2o system for 0.05 M $AlCl_3$ + 0.3 M HNO_3 concentration at 25^{o}C.

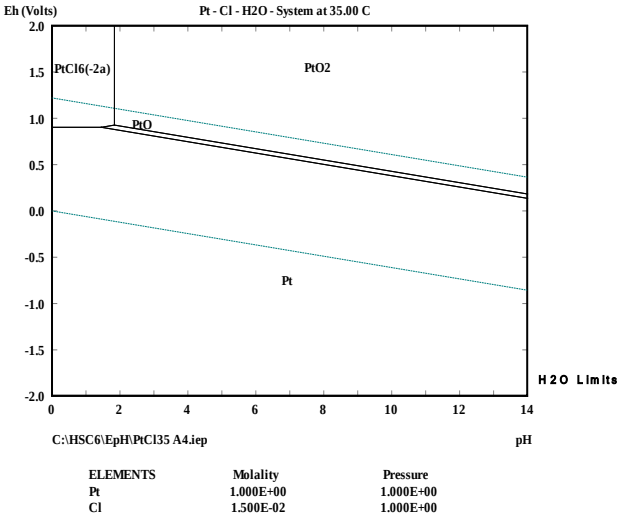

Figure D.3: E_h-pH diagram of Pt- Cl- H_2o system for 0.015 M $AlCl_3$ + 0.1 M HNO_3 concentration at 35^{o}C.

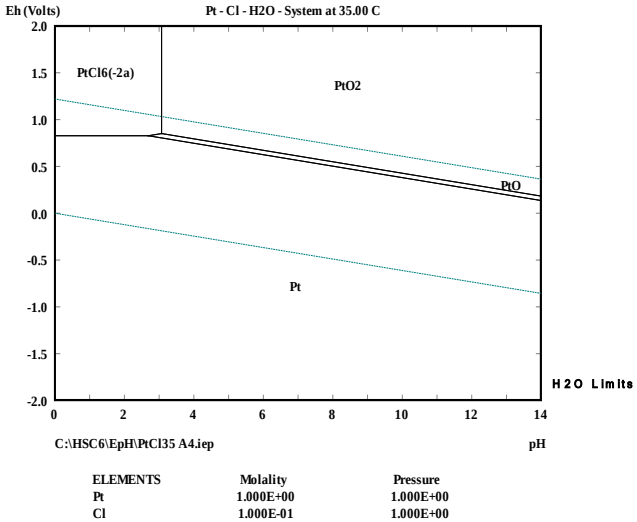

Figure D.4: E_h-pH diagram of Pt- Cl- H_2o system for 0.1 M $AlCl_3$ + 0.3 M HNO_3 concentration at 35^{o}C.

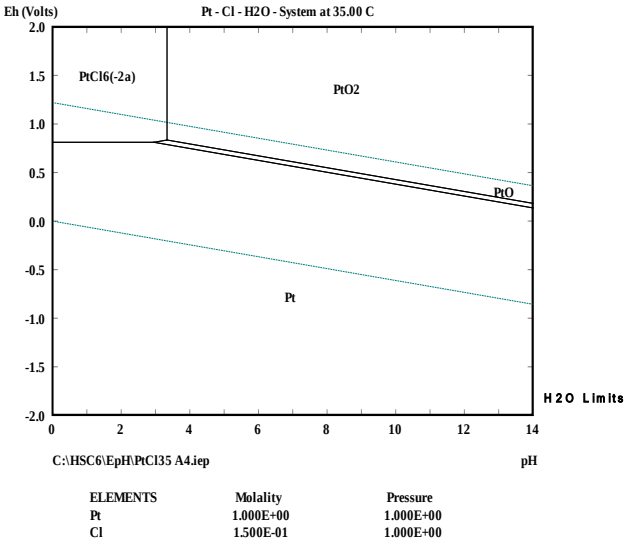

Figure D.5: E_h-pH diagram of Pt- Cl- H_2O system for 0.15 M $AlCl_3$ + 0.3 M HNO_3 concentration at 35°C.

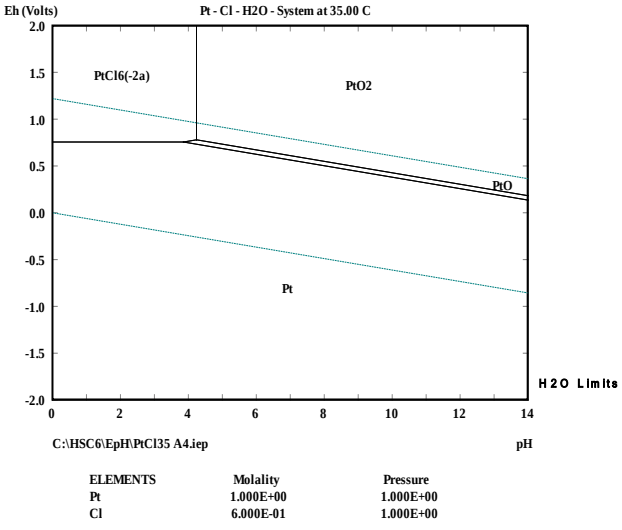

Figure D.6: E_h-pH diagram of Pt- Cl- H_2O system for 0.6 M $AlCl_3$ + 0.9 M HNO_3 concentration at 35°C.

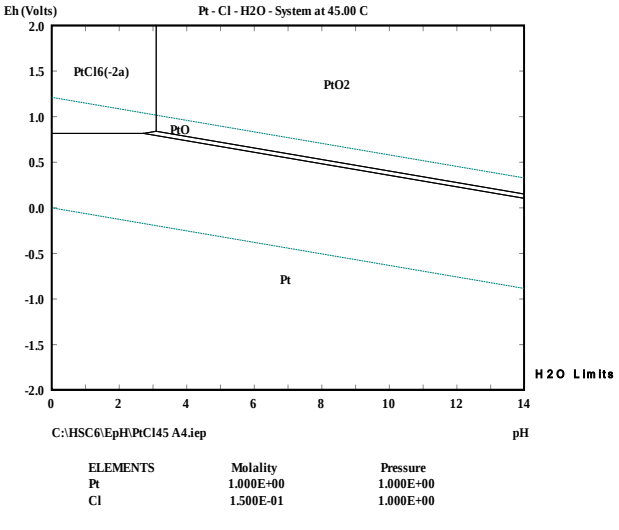

Figure D.7: E_h-pH diagram of Pt- Cl- H_2O system for 0.15 M $AlCl_3$ + 0.3 M HNO_3 concentration at 45°C.

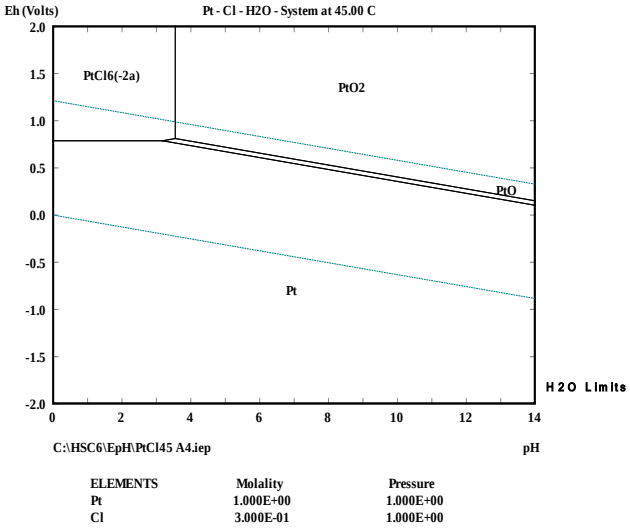

Figure D.8: E_h-pH diagram of Pt- Cl- H_2O system for 0.3 M $AlCl_3$ + 0.9 M HNO_3 concentration at 45°C.

Appendix E Polarisation curves on the influence of temperature of platinum

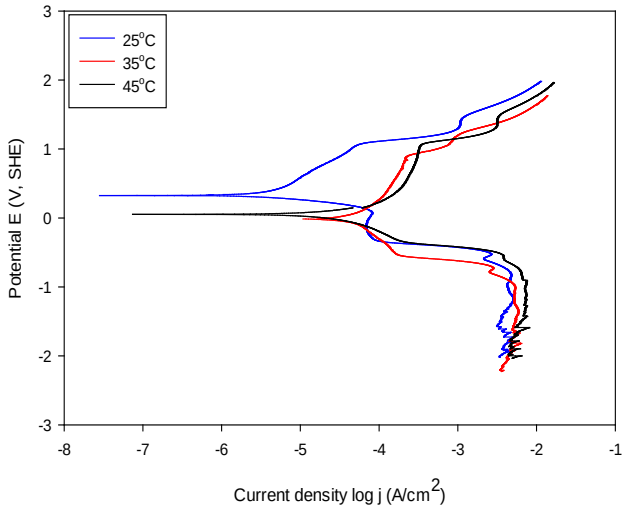

Figure E.1: Polarisation curves of Pt at 25, 35 & 45°C in 0.015 M $AlCl_3$ + 0.1 M HNO_3 after nitrogen deaeration.

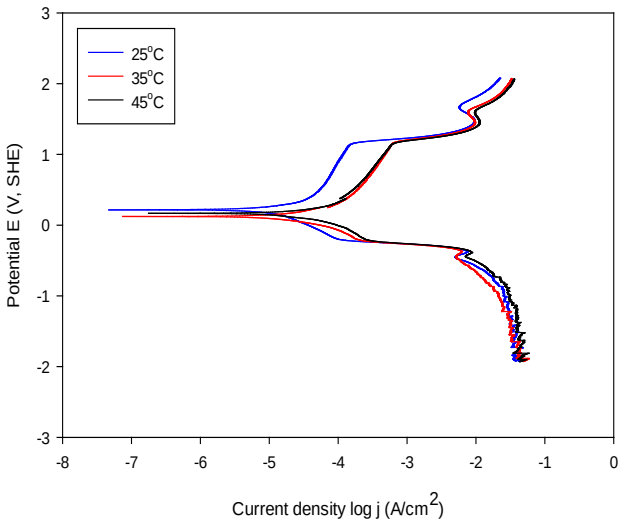

Figure E.2: Polarisation curves of Pt at 25, 35 & 45°C in 0.1 M $AlCl_3$ + 0.3 M HNO_3 after nitrogen deaeration.

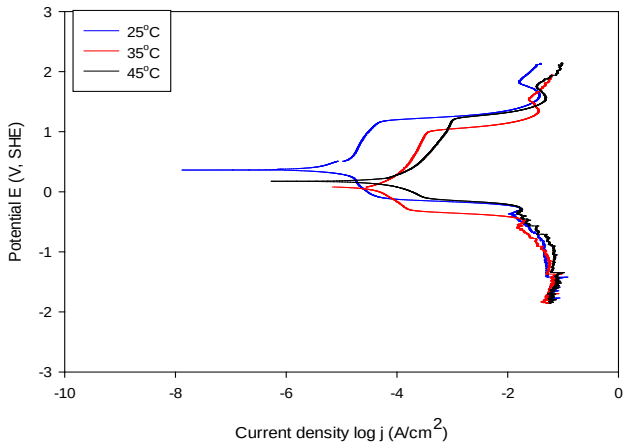

Figure E.3: Polarisation curves of Pt at 25, 35 & 45°C in 0.3 M $AlCl_3$ + 0.9 M HNO_3 after nitrogen deaeration.

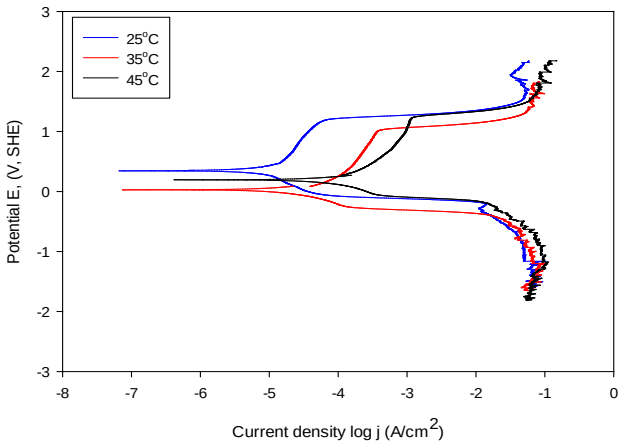

Figure E.4: Polarisation curves of Pt at 25, 35 & 45°C in 0.6 M $AlCl_3$ + 0.9 M HNO_3 after nitrogen deaeration.

Appendix F Polarisation curves on the influence of chloride ion concentration

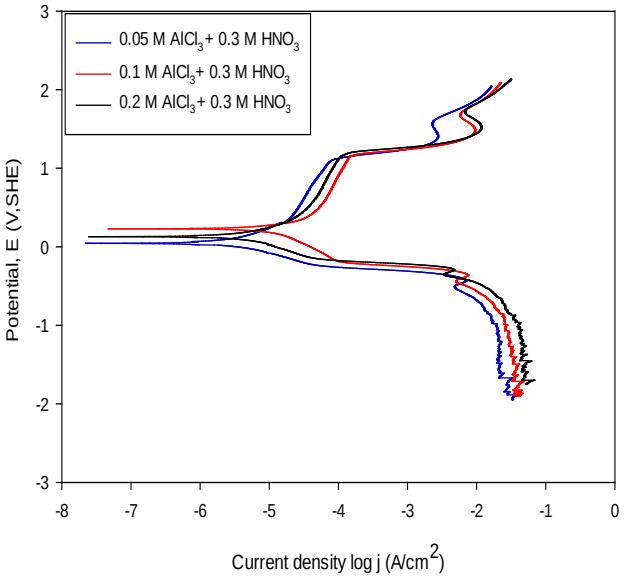

Figure F.1: Polarisation curve of Pt in 0.05, 0.1 & 0.2 M $AlCl_3$ + 0.3 M HNO_3 at 25°C.

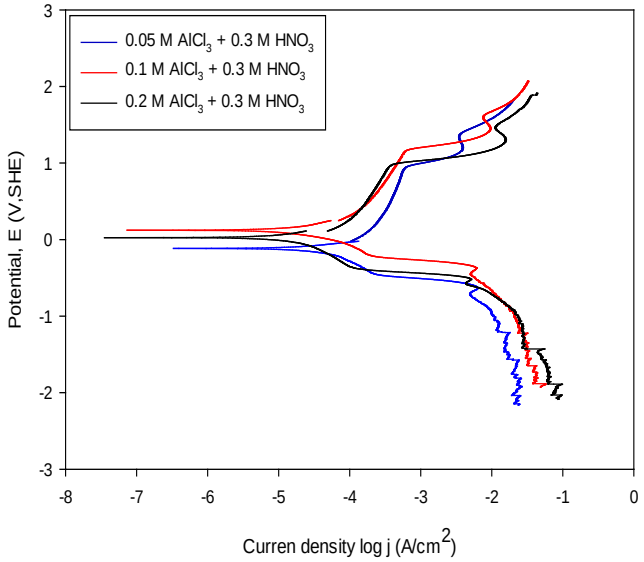

Figure F.2: Polarisation curve of Pt in 0.05, 0.1 & 0.2 M $AlCl_3$ + 0.3 M HNO_3 at 35°C.

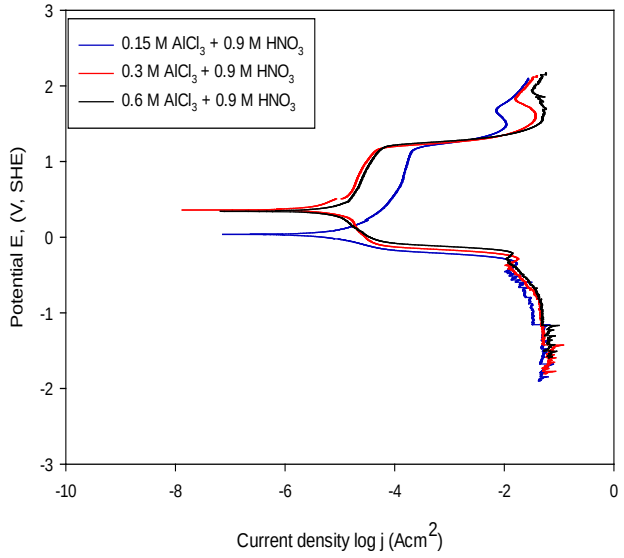

Figure F.3: Polarisation curve of Pt in 0.15, 0.3 & 0.6 M $AlCl_3$ + 0.9 M HNO_3 at 25°C.

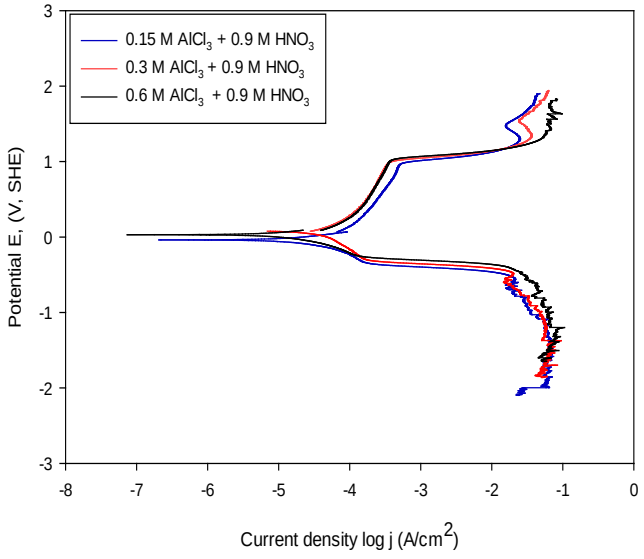

Figure F.4: Polarisation curve of Pt in 0.15, 0.3 & 0.6 M $AlCl_3$ + 0.9 M HNO_3 at 35°C.

Appendix G Summary of polarisation curves obtained experimentally

The selected experimental polarisation curves										
Temperature Conditions	**Contents**	**A**	**B**	**C**	**D**	**E**	**F**	**G**	**H**	**I**
25 °C	Figure no.	4.10, 4.11	4.9, 4.10	4.10	4.2			4.7*	4.8	4.3#, 4.6#
	Appendix	E1			F1	E2, F1	F1	F3	E3, F3	E4, F3
35 °C	Figure no.		4.9							4.4
	Appendix	E1			F2	E2, F2	F2	F4	E3, F4	E4, F4
45 °C	Figure no.	4.11	4.9, 4.11	4.11	4.12	4.12	4.8*, 4.12	4.13	4.13	4.13
	Appendix	E1				E2			E3	E4

with and without stirring * with and without deaeration

Legend: $AlCl_3$ + HNO_3: **A**: 0.015M+0.1M; **B**: 0.03M+0.1M; **C**: 0.06M+0.1M; **D**: 0.05M+0.3M; **E**: 0.1M+0.3M; **F**: 0.2M+0.3M; **G**: 0.15M+0.9M; **H**: 0.3M+0.9M; **I**: 0.6M+0.9M